

rec. August 4, 1976

A SLAC STREAMER CHAMBER PROPOSAL
TO STUDY
 ϕ MESON PRODUCTION MECHANISMS
AND
THE K^- ASSOCIATED LEPTON TO PION RATIO
AND
A SEARCH FOR CHARMED PARTICLE PRODUCTION
IN
 $\pi^+ p$ INTERACTION AT 15 GeV/c

Z. Ming Ma*, G. B. Thomson and J. Hylen
Michigan State University

and

R. H. Milburn, R. K. Thornton, F. T. Dao,
W. A. Mann and J. Schneps
Tufts University

SLAC

SEP 3 1976

LIBRARY

*Please direct all inquiries to:

Z. Ming Ma
Department of Physics
Michigan State University
East Lansing, Michigan 48824
Telephone: 517-355-4586

I PHYSICS JUSTIFICATION

(a) Production Mechanisms for ϕ -meson.

Since the discovery of ψ/J (3095) at BNL¹ and SLAC² there has been renewed interest in the assumption of a fourth quark, called the charmed quark (c for short). By now, there is strong credibility that the ψ/J (3095) is an orthocharmonium state³ with other higher mass enhancements being identified as excited states in this $c\bar{c}$ bound state picture. To complete this picture, it is absolutely necessary⁴ that mesons and baryons with a non-zero charm quantum number exist. Experimental searches for these charmed particles in hadronic reactions thus far have not turned up convincing evidence.⁵⁻⁸

In as much as ϕ (1019) is almost a pure $s\bar{s}$ state, it is very likely that production mechanisms for ϕ (1019) and ψ/J (3095) share many common features. Empirical rules governing ϕ (1019), such as Zweig's Rule, which was proposed to explain the suppression of ϕ decay into the $\rho\pi$ state may be applicable to ψ/J (3095). Although applicability of Zweig's Rule to production processes has not been unambiguously demonstrated, available experimental evidence seems to support such a notion, at least qualitatively. For example, in the reaction



Ayres⁹ observed that the reaction is suppressed relative to the reaction



by a factor of some 280. This is expected according to Zweig's Rule. Except for the ϕ meson, none of the other participants in the reaction carries a significant amount of the strange quark in its wave function. Therefore in terms of the standard particle exchange picture, the strange and the antistrange quark lines must terminate on themselves as is shown in

Figure 1 (a). This mechanism is suppressed according to Zweig's rule. For reaction (2) no such effect is expected. Furthermore, a comparison of the production cross-sections (see Figure 2) for reactions (1) and (2) enhances one's impression that these two reactions may indeed be governed by different mechanisms. The cross-sections for ϕ production exhibit a very steep drop-off ($\sigma \sim P_L^{-3.5}$) following a rapid rise from threshold. This is characteristic of Fermi's statistical model or a Regge cut model. In comparison, the ρ production cross-sections fall slowly with energies ($\sigma \sim P_L^{-1.89 \pm 0.09}$).

Suggestions have been made¹⁰ that Zweig's rule is strictly observed for ideally mixed vector and tensor meson states. The apparent violations such as reaction (1) are due to the mixing effect in the physical particles. It therefore, follows that the cross section ratio, R, is given by

$$R \equiv \frac{\sigma(\pi^- p \rightarrow \phi n)}{\sigma(\pi^- p \rightarrow \omega n)} = g_{\phi\rho\pi}^2 / g_{\omega\rho\pi}^2 = 1/225 \quad (3)$$

The cross section ratio is expected to be a constant. Although the cross section for the reaction



is poorly known, considerations of allowed exchange mechanisms would lead one to expect that reaction (4) (via ρ exchange) should have a slower energy-dependent fall off in cross sections than reaction (2) (via π exchange).

Taking this factor into consideration, one would conclude that the cross section ratio R decreases rapidly with increasing momentum, therefore, inconsistent with equation (3). Similar results have been reported by a Liverpool group¹¹ in a comparison of the reactions



at 3.6 GeV/c. Here the observed rate based on 12 events for reaction (6) is

an order of magnitude higher than would be expected from the measured rate for reaction (5).

Recently, a theoretical attempt to understand reaction (1) in terms of a double Regge pole exchange picture was advanced by Berger and Sorensen.¹² Figure 1 (b) shows the proposed exchange mechanism. The precipitous drop-off in the production cross sections is explained in terms of a cancellation effect by $K(890)$ and $K(1420)$ in the intermediate state. Although the model can account for the shape of the cross section drop-off, it fails to predict its experimental magnitude by a factor of 3. In addition, the model predicts a turn over in the t -distribution which is not observed experimentally.

On the constructive side, it was first pointed out by Sivers¹³ that one might expect to observe production of a pair of strange particles in association with the ϕ meson (Figure 3(a)). An example of this mechanism (Figure 3 (b)) would be



where the s and \bar{s} quarks from the ϕ meson terminate on the neighboring K^0 and Λ^0 respectively. Experimental data relevant to this question are quite limited. In $\bar{p}p$ interaction at 3.6 GeV/c, the cross section ratio is reported to be $\sigma(\bar{p}p \rightarrow \phi \pi^+ \pi^-) / \sigma(\bar{p}p \rightarrow \phi K^+ K^-) = 0.7 \pm .3$ (8)

based upon a total of 24 ± 4 ϕ events. An unpublished piece of information from the OMEGA Spectrometer group indicated¹⁴ that in the $\pi^- p$ interaction at 19 GeV/c, the cross section ratio is

$$\sigma(\pi^- p \rightarrow \phi \pi^+ \pi^- \pi^- p) / \sigma(\pi^- p \rightarrow \phi K^+ K^- \pi^- p) = 1.4 \pm .3 \quad (9)$$

based on a total of 120 ϕ events. In both cases, the ratios are consistent with being one. However, in both experiments, ϕ events represent a larger fraction of the final states when an additional pair of kaons are involved.

H. Lipkin¹⁰ has argued that the proper interpretation for experimental data such as (8) and (9) is complicated by the fact that it is difficult to produce a kaon pair in any reaction. Therefore, cross section ratios (8) and (9) merely indicate the relative difficulties for Zweig's rule violations as compared with producing an extra pair of charged kaons. Available data, therefore, seem to support the notion that these two processes are comparable in magnitude.

In summary, experimental facts on Zweig's rule are virtually nonexistent and our understanding of the dynamic origin of Zweig's rule is very limited. A careful study of ϕ producing reactions can not only shed light on the mechanism for producing a bound state of a pair of identical quarks, such as ϕ , f' (1520), ψ/J (3095), etc. in hadronic interaction, but also can provide a basis for understanding the dynamic origin of Zweig's rule. Furthermore, since ϕ production cross sections are of the order of $10^2 \mu\text{b}$, it makes sense to test dynamic models such as the associated production picture of Sivers (e.g. ϕ production in association with a pair of strange particles and ψ/J production in association with a pair of charmed particles) using the ϕ -meson before embarking on a massive search for charmed particles using ψ/J or ψ' mesons.

A survey of currently existing data indicates that except for reaction (1), data are virtually non-existent for exclusive ϕ production reactions where Zweig's rule may play an important role. In this experiment, we propose to use the trigger

$$\pi^+ p \rightarrow K^- + X \quad (10)$$

to obtain a large sample of ϕ events at a level of 144 to 436 events/ μb . This includes an acceptance of 5.7 to 17.2%.

(b) Search for New High Mass $K\bar{K}$ States

An effective K^- trigger will also make possible a high statistics search for new high mass $K\bar{K}$ states. One such state that is of particular interest here is the ϕ' , the missing member of the $J^P = 3^-$ nonet.¹⁵ It is expected that ϕ' should have a mass between 1800 and 1900 MeV/c^2 and has an appreciable decay rate into $K\bar{K}$ states. The triggering efficiency as a function of the $K\bar{K}$ mass is given in Figure 4. Here the $K\bar{K}$ pair is assumed to be isotropically produced. At a mass of 1800 MeV/c^2 , it is expected that a 120 to 360 event/ μb sensitivity can be achieved.

(c) Measurement of $R(e^+/\pi^+)$ with an Accompanying K^-

The subject of direct lepton production¹⁶ has been of interest for over ten years. Although specific emphasis has been shifting over the years, its general motivation is always to search for new particles, such as the intermediate vector boson W^\pm , recently discovered ψ/J (3095) and these elusive charmed particles.

Recent results from ISR^{17,18}, BNL¹⁹ and Fermilab²⁰⁻²⁴ indicate that in proton-nucleon or proton-nucleus interactions,

- (i) the ratio $R(\mu/\pi) \approx R(e/\pi)$ to a 40% accuracy.
- (ii) the lepton to pion ratio $R(\ell/\pi)$ is $\sim 10^{-4}$ for $P_\perp > 1.5$ GeV/c.
- (iii) for the lower p_\perp region, the ratio $R(\ell/\pi)$ rises to $\sim 4 \times 10^{-4}$ as $P_\perp \rightarrow 0$.
- (iv) the lepton charge symmetry is good to a 10-20% level.

Taking all existing data into consideration, Lederman¹⁶ concluded that such large lepton to pion ratios cannot be explained by the production of known particles. The approximate equality of muon and electron production and the lepton charge symmetry seem to indicate that the source of these leptons is a vector meson. If such were the case the mass of such a vector meson will have to be between 0.7 and 1 GeV/c² to be consistent with existing data. Another possible explanation would be due to the semileptonic decay of new unknown particles, such as the charmed mesons or baryons.

Theoretical estimates^{4,25} for the leptonic and semileptonic branching ratios for a charmed particle range from 5 to 20%. Assuming that the charm quantum number is conserved in strong interaction, the D meson (the pseudo scalar charmed meson) must be produced either in a pair or in association with a charmed baryon, e.g., C. In either case, one would expect leptonic charge symmetry in the final state. Since dominant decay modes of charmed particles involve a strange particle in the final state, one would expect the lepton to pion ratio to be substantially higher than 10^{-4} when the lepton is accompanied by a kaon.

Experimental evidence for anomalous direct lepton production in association with strange particles has been reported in neutrino-proton²⁶ and $\bar{p}p$ ²⁷ interactions. In a bubble chamber experiment, Canter *et al.*²⁷ have reported the observation of 10 $K_S^0 e^\pm$ candidate events in $\bar{p}p$ interaction at 15 GeV/c. A total of 9 of these events are identified by an e^+ or e^- shower behind a 2 radiation lengths tantalum plate placed in the BNL 80-inch hydrogen bubble chamber. The remaining candidate shows a characteristic e^- spiral in the bubble chamber. Background calculations indicate that only 1.5 events can be accounted for by hadronic showers and accidental correlations. These results come from a scan of 921 $K_S^0 \rightarrow \pi^+ \pi^-$ events. This corresponds to a production cross section $\sigma(K_S^0 e^\pm)$ of 13 μb and ratios of

$$R(K_S^0 e^\pm / \pi^\pm) = 1.2 \times 10^{-4} \quad (11)$$

and

$$R(K_S^0 e^\pm / K_S^0) = 9.3 \times 10^{-3} \quad (12)$$

Assuming equal participations of all kaon charge states, one has

$$R(K e^\pm / \pi^\pm) = 4.8 \times 10^{-4} \quad (13)$$

An interesting question would be to ask whether or not charmed or charm-like particle production is responsible for the anomalously large lepton to pion ratio. If charmed particles are at the source of this effect, one would

expect to see a similar effect in π^+p interaction. Therefore, a measurement of the K^-e^+/π^+ ratio in π^+p interaction can confirm the large $K_S^0 e^\pm$ effect in $\bar{p}p$ interaction. With a larger sample of Ke events, it will be possible to study the final state composition of these events.

Assuming equal production of K_S^0 and K_L^0 , one may expect

$$R(K^-e^+/K^-) = 4.7 \times 10^{-3} \quad (14)$$

in this experiment.

(d) Search for Charmed Particle Production in π^+p Interaction

Experimental effort in search for charmed particles has been largely in e^+e^- and nucleon-nucleon interactions. Recently, a narrow enhancement has been reported by the LBL-SLAC collaboration using SPEAR.^{28,29} The structure is observed at a mass of $1.87 \text{ GeV}/c^2$ and has a width between 10 and 20 MeV/c^2 . Neutral decay modes of this particle have been seen in the $K\pi$ and $K3\pi$ states²⁸ and hints of charged states in the $K2\pi$ mode are also reported.²⁹ If these effects are indeed due to charmed particles, one would expect to detect copious production of these states in hadronic interactions.

Previous searches for hadronic production of charmed states in exclusive channels



have been reported.^{6,8} In a bubble chamber experiment, the upper limit for reaction (15) with π^+ and p in the Δ^{++} state is reported to be $2.5 \mu\text{b}$ for a 95% confidence level. The corresponding upper limit for reaction (16) is set at $3.0 \mu\text{b}$. In both cases, a K_S^0 or a Δ^0 in the final state is required. An inclusive search for two body decay modes of neutral charmed states has been carried out by an MIT-BNL group⁵. A small acceptance two arm spectrometer is used to look for structures in two body states from pBe interaction at 30 GeV/c . The upper limits³⁰ for the product σ_B are of the order of 118 nb for observing a 3 standard deviation effect in the $K^+\pi^-$ state at $1.87 \text{ GeV}/c^2$.

It is a well-known fact that meson production is far more copious in the meson-nucleon interaction than it is in the nucleon-nucleon interaction.³¹

Threshold reactions such as reactions (15), (16) and

$$\pi^+ p \rightarrow \pi^+ p F^+ F^- \quad (17)$$

where $C^{++} \rightarrow \pi^+ p D^0$

$$\begin{aligned}
 D^0 &\rightarrow K^- \pi^+, & \bar{D}^0 &\rightarrow K^+ \pi^-, \\
 \bar{K}^0 \pi^0, & & K^0 \pi^0, \\
 K^- \pi^+ \pi^0, & & K^+ \pi^- \pi^0, \\
 \bar{K}^0 \pi^+ \pi^-, & & K^0 \pi^+ \pi^-, \\
 K^- \pi^+ \pi^-, & & K^+ \pi^- \pi^-, \\
 \bar{K}^0 \pi^+ \pi^- \pi^0, & & K^0 \pi^+ \pi^- \pi^0
 \end{aligned}$$

and $F^\pm \rightarrow K^\pm K_S^0$

$$K^+ K^- \pi^\pm \quad (18)$$

are possible candidates for the discovery of these charmed mesons and baryons.

The value of detecting charmed particle production in exclusive channels is clear. Ability to identify other participants in a given reaction not only can reduce the combinatorial problem in mass plots, but also allows one to study the dynamic mechanisms governing the production of these states. From available data, it is obvious that for three or more body decay modes, there is substantial

ground for improvement. An ideal detector for such a search must have a large solid angle coverage, be triggerable and have a demonstrated multi-track handling capability. We believe that our proposed experiment with a K^- trigger in the streamer chamber is a natural vehicle for such a search.

Theoretical estimates for associated charmed production cross sections have been made by Field and Quigg³² and Barger and Phillips³³ separately using Regge pole models. For two body reactions, cross sections of the order of a nanobarn are predicted. Lee, Gaillard and Rosner⁴ argued that $D\bar{D}$ and $C\bar{C}$ pairs can result from the decays of high mass meson and baryon clusters respectively. Since these clusters may be produced diffractively in π^+p interaction, cross sections for the reaction

$$\pi^+p \rightarrow M + \dots\dots\dots (19)$$

$$| \rightarrow D^0 \bar{D}^0$$

or

$$\pi^+p \rightarrow N^{*++} + \dots\dots\dots (20)$$

$$| \rightarrow C_1^{++} \bar{D}^0$$

may be of the order of microbarns. Currently no positive information exists for charmed particle production in hadronic interactions. It is therefore, not possible to predict with confidence the energy dependence of cross sections for the production. However, one can argue that in general, cross sections for reactions requiring a quantum number exchange fall with increasing c.m. energy. On the other hand, the suppression due to large t_{min} or small available phase space near threshold would suggest that the production cross section should peak near but above the threshold energy. Furthermore, experimental evidence³¹ seems to support the notion that mesons tend to be produced more copiously with a meson beam than with a baryon beam. Therefore, our proposed experiment should provide an interesting ground for charmed particle searches.

II EXPERIMENTAL SETUP

The proposed set up is shown in Figure 5. A 15 GeV/c π^+ beam is incident upon a 60 cm liquid hydrogen target placed at the center of the streamer chamber. The K^- trigger is shown to the right of the beam line. Three sets of vertical picket fence counters are placed at 2,3 and 4 meters downstream of the target. These are designated as V_{1i} , V_{2i} , and V_{3i} ($i = 1,2,\dots,15$). The first array is composed of 15 counters, each measuring 5 cm wide by 40 cm high. The left edge of V_{11} is placed on the center line of the streamer chamber. Counters of the second array are 7.5 cm wide by 60 cm high and are placed 3.75 cm to the right of the center line. The third array is shifted 10 cm to the right and each element measures 10 cm by 80 cm.

Immediately downstream of the V_{3i} array is a multicell high pressure threshold \bar{C} erenkov counter. The counter is 1 m long and has 10 mirrors at the back in the form of a 2x5 matrix covering an area of 2 m wide by 1 m high. It will be capable of handling 3 atmospheres of Freon 12 and will have better than 99% efficiency for pions of 2 GeV/c or above. Detailed design considerations are given in Appendix I. A fourth array of 15 counters V_{4i} , ($i = 1,2,\dots,15$) are deployed immediately behind the \bar{C} erenkov counter. Each counter measures 12.5 cm wide by 100 cm high and covers the same solid angle as the corresponding upstream counter.

The e^+ tagging system is seen on the left hand side of the beam line. It consists of an 80 cm wide by 1.45 m high by 1 m long atmospheric pressure CO_2 \bar{C} erenkov counter covered at the upstream side by a set of 10 scintillation counters, C_i with an area of 30 cm wide by 75 cm high and followed by a shower detector E_i placed at 3 m downstream of the target. The likely configuration for the shower detector is to be composed of 80 modules of lead-glass \bar{C} erenkov counters, each has a 6.35 cm x 6.35 cm cross section by 58.4 cm long. These

counters will be grouped into two blocks, covering an area of 1.168 m high by 58.4 cm wide. Each block consists of 4 layers of 10 counters arranged in a cross-hatch pattern. The lead-glass counters are backed up by a set of 20 modules of lead-scintillator sandwich shower counters covering an area of 60 cm by 1.25 m. The detailed descriptions of the \bar{C} erenkov counter and the shower counters are given in Appendices II and III respectively. The right edges of both the \bar{C} erenkov counter and the front scintillation counters C_i are displaced 20 cm to the left of the center line. The shower counter starts at 30 cm to the left of the center line. Pulse height information from the shower counters will be recorded on tape for off-line analysis.

The trigger for this experiment will be

$$K^- = \pi^+ \cdot (\sum_i V_{1i} \cdot V_{2i} \cdot V_{3i} \cdot \bar{C}_{\pi i} \cdot V_{4i}) \quad (21)$$

The tagging logic for the e^+ will be

$$e^+ = K^- \cdot (\sum_i C_i \cdot \bar{C}_{e i} \cdot E_i) \quad (22)$$

III YIELD AND BACKGROUND ESTIMATES

The total π^+ p cross section at 15 GeV/c is³⁴ $24.05 \pm .28$ mb. A 60 cm long target corresponds to a 5.88% probability that an incident π^+ will interact in the liquid hydrogen. With 8 π^+ /pulse one has 0.47 interaction/pulse. In 300 hours, this experiment will have an equivalent sensitivity of 2.54 event/nb at 120 pps. But when acceptance is taken into consideration, the sensitivity is reduced by about one order of magnitude.

1. K^- Trigger

The trigger logic $\pi^+ \cdot (\sum_i V_{1i} \cdot V_{2i} \cdot V_{3i} \cdot V_{4i})$ defines that a negative charged particle is produced. Since the system is designed to trigger on a K^- from an incident π^+ , two dominant sources of strange particle production are eliminated: (a) the associated production by strangeness conservation and (b) diffraction production of A_2^+ and its subsequent decay into K^+K^0 pair.

Therefore, the only other source of K^- would be $K^-\bar{\Lambda}$ N or $K^-\bar{\Sigma}$ N. Available data from a bubble chamber experiment³⁴ indicate that this contribution is small ($< 50 \mu\text{b}$). Therefore for the purpose of the yield discussion, we shall assume that all K^- triggers have an associated K^+ and that a majority of the K^+K^- pairs will be from the decay of ϕ -mesons. Monte Carlo studies indicate that the acceptance is 5.7% for an isotropic production of ϕ -mesons in the center of mass system. The acceptance increases to 17.2% if the ϕ is produced according to e^{-4t} . Figures 6 (a,b) show the acceptance in the grand center of mass system for an isotropic production. Good efficiency is expected for forward produced ϕ -mesons. The peak in the azimuthal angular plot is due to the fact that the picket fence counters are deployed to the right of the center line. Figures 6(c,d) show the acceptance for K^- in the ϕ c.m. system. No void region is seen, thus indicating that the true decay angular distribution can be obtained. Figure 7 gives the geometric detection efficiency for the

K^- meson as a function of the Feynman X and P_{\perp} . Turning to triggering cross sections, one notes that there exists no reported data on either ϕ or K^- inclusive cross sections for π^+p interactions at 15 GeV/c. Experimental results at 300 GeV/c indicate that³¹ the inclusive ϕ cross section is about 250 μb . At 24 GeV/c, ϕ inclusive production in pp interaction³⁵ has a cross section of 175 μb . Inclusive neutral strange particle cross sections from Columbia data³⁴ on π^+p at 15 GeV/c suggest that the $K_S^0 K_L^0$ cross section can be as high as 540 μb . For a conservative estimate on the yield, we shall use 200 μb for inclusive ϕ production. This means in 300 hours, we can expect

$$2.54 \text{ event/nb} \times 200 \mu\text{b} \times 1/2 \times 5.7\% = 1.44 \times 10^4 \text{ events}$$

for an isotropic production. If the slope parameter is 4 GeV^{-2} , the yield becomes 4.36×10^4 events.

2. π^- Background Trigger

Monte Carlo studies using experimental data³⁴ on

$$\pi^+ p \rightarrow \pi^- + \text{anything} \quad (23)$$

at 15 GeV/c indicate that a 17.6% acceptance is expected for π^- based on the trigger logic

$$\pi^+ \cdot \sum_i V_{1i} \cdot V_{2i} \cdot V_{3i} \cdot V_{4i}$$

Figure 8 shows the π^- acceptance as a function of P_{\perp}^2 and X . The total inclusive π^- cross section is $24.50 \pm .34 \text{ mb}$, therefore, without the \checkmark Cerenkov counter, the expected π^- to K^- ratio would be

$$R(\pi^-/K^-)_{\text{no } \checkmark} = 24.50 \times 17.6\%/100 \times 10^{-3} \times 5.7\% = 7.6 \times 10^2 \quad (24)$$

Using the design specification for the high pressure \checkmark Cerenkov counter as is discussed in Appendix I, the noise to signal ratio is reduced to

$$R(\pi^-/K^-)_{\checkmark} = 0.019\% \times 24.50/100 \times 10^{-3} \times 5.7\% = 0.82 \quad (25)$$

for an isotropic production of ϕ - meson at 200 μb . If the slope parameter is 4 GeV^{-2} , this ratio becomes 0.27.

3. Random Veto of K^- Triggers by π^+ or π^-

A proper K^- trigger may be accidentally vetoed by a π^+ or π^- entering the same \checkmark Cerenkov cell. The probabilities for a π^+ or π^- hitting a 1 m by 2 m area at the mirror plane are 3.8% and 33.7% respectively. Since the inclusive cross sections for π^+ and π^- are $61.34 \pm .73$ mb and $24.50 \pm .34$ mb respectively, the averaged number of accidental π^\pm is given by

$$(61.34 \times 3.8\% + 24.50 \times 33.7\%) / 24.05 = 0.45.$$

If the \checkmark Cerenkov counter is divided into 5 distinct cells and the π^\pm veto occurs at random, the probability for a lost K^- trigger is $0.44/5$ or 8.8%.

4. π^+ Background in e^+ Tagging

The geometric acceptance for π^+ is expected to be 10.2% according to a Monte Carlo study. The experimental value of the π^+ inclusive cross section is $61.34 \pm .73$ mb. Since the overall beam intensity corresponds to 2.54 event/nb and we propose to trigger on

$$200 \times 1/2 \times 5.7\% \times (1-8.8\%)/24.05 \times 10^3 = 2.16 \times 10^{-2}\% \quad (26)$$

of all interactions, one can expect

$$2.54 \times 10^6 \times 61.34 \times 10.2\% \times 2.16 \times 10^{-2}\% = 3.44 \times 10^3 \pi^+ \quad (27)$$

Using the e^+ tagging system as is described in Appendices II and III, a pion rejection inefficiency of 5×10^{-4} can be expected. Therefore, as many as $2 \pi^+$ may be mistagged as e^+ .

5. e^+ Tagging

To date, we are unaware of experimental data on e^+ inclusive distributions from π^+p interactions. In the acceptance calculation, e^+ is assumed to follow the same x and P_{\perp}^2 distributions as π^- . Monte Carlo studies show that 13.5% of the e^+ thus produced will be tagged by the system. Figure 9

shows the e^+ acceptance as a function of Feynman X and P_{\perp} . As may be seen, this experiment is particularly sensitive to the low P_{\perp} region where lepton to pion ratio is expected to rise above the asymptotic value of 10^{-4} .

If the lepton to pion ratio remains at the 10^{-4} level for π^+p interaction, we should have 0.5 e^+ taggings. On the other hand, if the anomalously high K_S^0 associated e^+ rate seen by the Tufts group represents new physics, such a rate should also prevail in π^+p interaction. Using a reasonable assumption

$$R(K^-e^+/K^-)_{\pi^+p} = 1/2 R(K_S^0 e^{\pm}/K_S^0)_{p\bar{p}} = 4.7 \times 10^{-3} \quad (28)$$

one can expect 8 to 25 e^+ taggings taking into account the e^+ acceptance of 13.5%. Since e^+ taggings due to normal prompt lepton production is small, any significant e^+ signals will represent interesting new physics.

6. e^+ Background Tagging

Background positron contamination can come from either γ -ray conversions in material or Dalitz pairs at the interaction vertex.

(a) External Conversions. Although external conversions can be eliminated from data sample by extrapolating charged tracks to the Čerenkov counter and the lead glass detector, these taggings do resemble legitimate showers for the shower detectors. To estimate this source of background, the following amounts of material are used

- a. Aluminum ground flap: 1/32",
- b. Foam wall surrounding the sensitive volume of the chamber:
1" with $\rho = 0.15$ gm/cc,
- c. 10 mil stainless steel
- d. target material: 1 mm with $\rho = 0.1$ gm/cc

A total of 0.06 radiation length is used. The acceptance for a e^+e^- pair can be estimated assuming isotropic distribution for the γ -rays. The total inclusive π^0 cross section³⁴ is 32.91 ± 1.20 mb and the total solid angle subtended by the lead-glass array at the target is $58.4 \times 127/300^2 = 0.0066 \times 4\pi$. Therefore, ignoring positron bending by the magnetic field, we get

$$2 \times 32.91 \times 0.0066 \times 0.06 = 2.6 \times 10^{-2} \text{ mb} = 26 \text{ } \mu\text{b}$$

Referring to calculations done for π^+ background tagging, we expect

$$2.6 \times 10^{-2} \times 2.54 \times 10^6 \times 2.16 \times 10^{-2}\% = 14 \text{ } e^+ \text{ taggings.}$$

(b) Dalitz Pairs. The acceptance for a positron from an internally converted γ -ray is 9.4% and 8.8% for a lead glass array of 58.4 cm x 1.27 m and 58.4 cm x 63.5 cm surface area respectively. Using the π^0 inclusive cross section of 32.91 ± 1.20 mb and the 1/80 probability for internal conversions, we expect

$$9.4\% \times 32.91 \times 1/80 \times 2.54 \times 10^6 \times 2.16 \times 10^{-2}\% = 21 \text{ } e^+ \text{ taggings.}$$

One notes that a great majority of these taggings can be eliminated off line by a cut on e^+e^- invariant mass. There is a small component of it that cannot be weeded out, i.e. if the e^- has such a low momentum that it is concealed in the target assembly. For the purpose of this calculation, we assume that for momentum less than 10 MeV/c, the pair will appear as a single e^+ . This corresponds to a 0.2% probability or 0.04 e^+ tagging. A summary of triggering and tagging statistics is given in Table 1.

7. Sensitivity for Charmed Particle Production

(a) Exclusive Channels. A Monte Carlo study for reaction (15) has been made. Assuming that D^0 has a mass of $1.87 \text{ GeV}/c^2$, the acceptances for $D^0 \rightarrow K^- \pi^+$, $K^- \pi^+ \pi^0$ and $K^- 2\pi^+ \pi^-$ are 6.9, 9.8 and 10.2% respectively.

Therefore this proposed experiment will have a sensitivity on $\sigma \cdot B$ of 175 to 260 event/ μb .

(b) Inclusive Charmed Particle Search. The sensitivity for an inclusive charmed particle search is somewhat complicated. It depends on the decay modes of D^0 and \bar{D}^0 and the topology of the final state. To illustrate the point, let us consider reaction (15), $\pi^+ p + \pi^+ p D^0 \bar{D}^0$ in which $D^0 \rightarrow K^- \pi^+$ and $\bar{D}^0 \rightarrow K^+ \pi^- \pi^0$. This event falls in the 6 prong topology. Since K^- is identified by the Čerenkov counter, it only remains to pick the proper π^+ for the invariant mass calculation. Assuming that the proton is identified by the ionization technique or other means, one is left with 3 combinations. Therefore, each event will enter 3 times into the $K^- \pi^+$ mass plot. If the K^- associated topological cross sections follow the same trend as those of the overall reaction, a 6 prong event ($\sigma = 5.06 \pm .12 \text{ mb}$) should occur 21% of the time. For a 43600 event sample (for a ϕ slope of 4 GeV^{-2}) one has 9170 6 prong events or 27,510 entries into the $K^- \pi^+$ mass plot. The total available phase space at 15 GeV/c is about $3 \text{ GeV}/c^2$. Therefore, on the average one has 9.2 entries/MeV/c². Assuming a 1% $\Delta m/m$ resolution, the D^0 peak will be resting on a 171 event background. For a 3 standard deviation effect, one needs $3\sqrt{171}$ or 39 events. This corresponds to a $\sigma \cdot B$ sensitivity = $39/2.54 \times 6.9\% = 225 \text{ nb}$. Similar exercises have been done for other decay modes and are given in Table 2. As may be seen, the $\sigma \cdot B$ sensitivity in this experiment varies between 50 and 250 nb for a 3 standard deviation effect. Observation of such an effect in several different channels can surely reinforce one's confidence that these are not due to statistical fluctuations. This is about an order of magnitude improvement over previous bubble chamber experiments. Furthermore, the present capability of a streamer chamber to handle a multi-track event should

offer assurance of success at this sensitivity level.

IV DEAD TIME CONSIDERATION

Due to the low trigger rate in this experiment, dead time losses would be minimal. As may be seen in Table 1, the expected number of triggers is 24 K to 50 K. Allowing for 150 K pictures and 300 millisecond for film advance, the dead time losses amount to 4.17% of the available beam.

V SUMMARY OF REQUESTS

1. Beam: π^+ at 15 GeV/c
 - a. Momentum and angular dispersions: $\Delta p/p = \pm 3/4\%$ for a beam spot of 6mm FWHM at the center of the streamer chamber. Angular divergence better than ± 2 mr will be desirable.
 - b. Intensity: $7 \pi^+$ per pulse at 120 pps for data run.
2. Machine Time: 300 hours at 120 pps for data run and 500 hours at 10 pps for set up and equipment testing.
3. Liquid Hydrogen Target: A 60 cm long liquid hydrogen target with ~ 1 cm diameter cross section is needed.
4. Fast Electronic Logic: Parts of the fast logic needed in this experiment will be borrowed from the SLAC equipment pool.
5. Cerenkov counters:
 - a. A high pressure Freon 12 \checkmark Cerenkov counter with its associated gas circulation and pressure monitoring systems is needed for K^- trigger. For detailed specifications see Appendix I.
 - b. A low pressure CO_2 \checkmark Cerenkov counter with its associated gas circulation and pressure monitoring system is needed for e^+ tagging. For detailed specification, see Appendix II.
6. Computer Time: Processing for up to 2000 streamer chamber events through the SLAC-LBL SIOUX reconstruction-fitting routine is requested.
7. Scanning and Measuring Facilities: Nominal access to the SLAC scanning and measuring facilities for system check out is needed. Measuring for up to 2000 events is requested.
8. Film: up to 150 K triads will be needed.
9. Beam Track Measurement: 3 modules of PWC of 2mm wire spacings with associated amplifiers are needed for beam direction definition.

TABLE 1. A SUMMARY OF EXPECTED TRIGGERS AND TAGS

ϕ Production Slope, b (GeV^{-2})	0	4
<u>K⁻ Trigger</u>	<u>1.31×10^4</u>	<u>3.92×10^4</u>
Number of K ⁻ Triggers	1.44×10^4	4.36×10^4
Random Veto by π^{\pm}	$.13 \times 10^4$	$.38 \times 10^4$
<u>π^- Trigger</u>	<u>1.07×10^4</u>	<u>1.06×10^4</u>
<u>e⁺ Tagging</u>	<u>43</u>	<u>132</u>
K ⁻ Associated	8	25
External Conversion	14	43
Dalitz Pair	21	64
$P_{e^-} < 10 \text{ MeV/c}$	0.04	0.12
<u>π^+ Tagging</u>	<u>2</u>	<u>5</u>

TABLE 2a. TOPOLOGICAL CROSS SECTIONS

Topology	Cross Section (mb)	% of σ_{total}	$\frac{\text{No. of events}}{43600 \text{ total events}}$
2	$8.16 \pm .16$	33.93	14800
4	$9.26 \pm .18$	38.51	16790
6	$5.06 \pm .12$	21.04	9170
8	$1.33 \pm .04$	5.53	2400
10	$0.21 \pm .01$	0.87	380
12	$0.024 \pm .003$	0.10	44
14	$0.003 \pm .001$	0.01	4
Total	$24.05 \pm .28$	100.0	

TABLE 2b. UPPER LIMITS (IN NANOBARN) FOR OBSERVING A 3 STANDARD DEVIATION EFFECT IN $\pi^+ p \rightarrow \pi^+ p D^0 \bar{D}^0$

	D^0 Decay Mode					
	$K^- \pi^+$	$\bar{K}^0 \pi^0$	$K^- \pi^+ \pi^0$	$\bar{K}^0 \pi^+ \pi^-$	$K^- \pi^- \pi^+ \pi^-$	$\bar{K}^0 \pi^+ \pi^- \pi^0$
D^0 $K^+ \pi^-$	225	NT	158	NT	110	NT
D^0 $K^0 \pi^0$	248	NT	UC	NT	152	NT
D^0 $K^+ \pi^- \pi^0$	225	NT	UC	NT	110	NT
D^0 $K^0 \pi^+ \pi^-$	225	NT	158	NT	110	NT
D^0 $K^+ \pi^+ \pi^- \pi^-$	133	NT	94	NT	57	NT
D^0 $K^0 \pi^+ \pi^- \pi^0$	225	NT	UC	NT	110	NT

NT = not trigger the system

UC = underconstrained, multi-neutral particles
in the final state.

APPENDIX I. HIGH PRESSURE \checkmark CERENKOV COUNTER FOR π^- VETOES

1. Basic Considerations

The trigger logic $\pi^+ \cdot \sum_i V_{1i} \cdot V_{2i} \cdot V_{3i} \cdot V_{4i}$ effectively defines a negatively charged particle. The momentum distributions for the K^- and π^- accepted by this logic are given by Figures A.I.1 (a and b) respectively. The π^- sample is generated using experimental data whereas K^- curve assumes an isotropic production of ϕ - meson in the c.m. Corrections for decays in flight have been applied to the K^- spectrum only. Since π^- inclusive cross section is $24.50 \pm .34$ mb, it is of overriding importance that the \checkmark Cerenkov counter can effectively veto virtually all of the π^- accepted by the picket fence counter logic. Since the ratio of the threshold momenta for π^- and K^- is equal to the inverse of the mass ratio, it is not possible to save all K^- triggers and at the same time veto all π^- particles. A minimum of 99% efficiency for vetoing π^- with 2 GeV/c is chosen for the design. Using standard formulas for \checkmark Cerenkov counters^{36,37}

$$\cos \theta = \frac{1}{\beta n} \quad (\text{A.I.1})$$

and

$$N = 2\pi\alpha \ell \sin^2 \theta \int \frac{E(\lambda) f(\lambda, p) d\lambda}{\lambda^2} \quad (\text{A.I.2})$$

where N is the number of photoelectrons, β and θ are the velocity and the \checkmark Cerenkov angle of the charge particle, n and ℓ are the index of refraction and the path length of the particle in the gas. The quantity $E(\lambda)$ is the quantum efficiency of the photomultiplier tube. The function $f(\lambda, p)$ is the transmittance for \checkmark Cerenkov light of wavelength λ in a gas of pressure p . Its dependency on the pressure is given by³⁸

$$f(\lambda, p) = f(\lambda, p = 1 \text{ atm.})^\rho p / \rho_1 \quad (\text{A.I.3})$$

where ρ_p and ρ_1 are the density of the gas at a pressure p and 1 atmosphere respectively. The index of refraction of the gas as a function of the pressure is given by E. R. Hayes et. al.³⁹

The rapid drop-off in the number of photoelectrons with increasing wavelength suggests that the light collection system should be designed to accept as low a wavelength as one practically can. Figure A.I.2 shows the expected number of photoelectron, N as a function of pion and Kaon momenta for a specific design. Light losses in the collection stage are not included here. The specifications are given in Table A.I.1. It is expected that with a collection efficiency of 25%, one can achieve a pion detection inefficiency better than 10^{-3} at 2 GeV/c.

Cost estimates for such a high pressure \bar{v} Cerenkov counter have been made. Since the technical requirements can be met by two existing units at SLAC, we have essentially obtained reproduction costs for these counters. The two units are the C2 used in LASS⁴⁰ and CANUTE⁴¹ used in the 1 meter hybrid bubble chamber facilities. The cost for constructing a duplicate of the C2 \bar{v} Cerenkov counter is estimated by Al Kilert to be ~\$100K including phototubes but not associated electronics. For the CANUTE counter, the price is ~\$135K according to Clive Field. Both are in 1976 dollars. In Table A.I.2, a comparison of the counters is made. As may be seen, placed at 4 m downstream from the target these three units have almost identical solid angle acceptance.

It is the intention of this collaboration to borrow one of the existing counters. If all fails, we intend to request funds from ERDA, NSF and SLAC to construct such a counter. Needless to say, such a large aperture \bar{v} Cerenkov

counter will be very useful for a wide variety of experiments than can be done using the Streamer chamber facilities.

TABLE A.I.1 SPECIFICATIONS FOR A HIGH PRESSURE ^VCERENKOV
COUNTER

Physical Dimension: 1 m high x 2 m wide x 1 m long

Mirrors: 10 spherical mirrors in 2 x 5 matrix form covering an area of 1m x
2m at the downstream wall of the counter.

Photomultiplier Tubes: 10 units of Amperex 58 UVP

Gas and Pressure: Freon 12 up to 3 atmospheres.

Optical Consideration: All components in the light collection stage must be
designed with high transmission efficiency for
wavelength as low as 2200 Å, the cut off wavelength
for Freon 12.

v
TABLE A.I.2. COMPARISON OF THREE HIGH PRESSURE CERENKOV COUNTERS

	C2-LASS	CANUTE-SHF	Proposed
Reference	(40)	(41)	This Appendix
Physical Dimension (m ³)		3.55m diameter by 4.06m wide	
Radiator Length (m)	1.75m min.	2.93m	1m
Number of Mirrors	8	10	10
Total Mirror Surface	2.5m x 1.25m	2.75m x 1.40m	2m x 1m
Photomultiplier Tube	Amperex 58 UVP	Amperex 58 DVP	Amperex 58 UVP
Optical Pressure Window	Quartz	Acrylic coated with paraterphenyl (pTP)	Quartz
Beam entrance window size material	1m x 2.5m 2mm Al	2.04m x 1.02m 5.7 mm	0.8m x 1.6m
Inefficiency for pions	10 ⁻⁴ at 8 GeV/c for a 16.5 p.s.i.a Freon 12 gas	1.3x10 ⁻² at 14. GeV/c for a 22 p.s.i.a Freon 12 gas	10 ⁻³ at 2 GeV/c expected at 43 p.s.i.a.
Maximum Pressure	3 atmosphere	4 atmosphere	3 atmosphere

APPENDIX II. AN ATMOSPHERIC PRESSURE ČERENKOV COUNTER FOR e^+ TAGGING

The role of this low pressure Čerenkov counter is to signal the presence of an electron or an positron. Table A.II.1 gives the specifications for such a device. The momentum distributions for π^+ and e^+ that will satisfy the counter logic

$$\pi^+ \cdot \sum_i C_i \cdot E_i \quad (\text{A. II. 1})$$

are shown in Figure A. II.1. The π^+ distribution is generated according to the experimental data and the e^+ is assumed to follow that of π^- in both x and P_{\perp}^2 . The expected photoelectron yield from the Čerenkov Counter is shown in Figure A.II.2. Here the light collection efficiency is not included. It is expected that with CO_2 operated at one atmosphere and assuming a 25% light collection efficiency, this counter will be 50% efficient for a π^+ at 5.4 GeV/c. The overall effect of this Čerenkov counter is that it will reduce the acceptance of π^+ in the system from 10.2% to 1.7%. And the π^+ contamination is entirely from 5 GeV/c and above.

It should be noted that the upstream side of this counter is placed very close to the magnet coil, therefore, conventional light collection at this end is not possible. One possibility would be to reflect the Čerenkov light vertically by a mirror and place phototubes above and below the counter.

TABLE A.II.1 SPECIFICATION FOR AN ATMOSPHERIC PRESSURE ^VCERENKOV COUNTER

Physical Dimension: 80 cm wide by 1.45 m high by 1 m long

Mirrors: 4 spherical mirrors in 2 x 2 matrix form covering an area of 0.6 m x 1.30 m at the downstream wall of the counters

Photomultiplier Tubes: 4 units of Amperex 58 UVP

Gas and Pressure: CO₂ at 1 atmosphere

Optical Consideration: all components in the light collection stage must be designed with high transmission efficiency for wavelength as low as 2200 Å.

APPENDIX III. ELECTRON SHOWER COUNTER

The overall electron tagging system should discriminate in favor of single 1-8 GeV/c e^+ 's in the presence of a background of π^+ 's up to 10^4 times the e^+ flux. We propose to use for this purpose an existing hodoscope array consisting of 60 (and possibly 80 to double the solid angle coverage) Pb-glass blocks (Schott SF-2) each $6.35 \times 6.35 \times 58.4 \text{ cm}^3$, with attached Amperex XP2020 photomultipliers, and associated calibration pulsers and CAMAC/PDP-11 read-out system.⁴²

The primary background comes from the hadronic interactions of pions in the glass which lead to π^0 production and decay and to a continuum of electromagnetic shower energy deposition in the remainder of the counter. This problem has been studied in detail by Blumenfeld et al⁴³ who observed, typically, at 8 GeV the pulse-height spectrum shown in Figure A.III.1 in a configuration of SF-5 glass measuring 43.7 cm (18.7 rad. len.) along a mixed pion-electron beam. Using only the total pulse from the counter they found they could discriminate electrons from pions at the same known momentum down to a level of about 10^{-2} , as is qualitatively evident from the figure. They also found that by measuring separately the pulse height in the front 1/3 of the counter radiator (about 6 rad. len.) in which the electron is more likely to have begun showering than the pion, an additional discrimination against the latter could be made. The improvement depends on the choice of discriminator setting for the first segments, and must represent a compromise between pion rejection and loss of efficiency for electrons. In an experimental counter built along these lines at CERN-ISR, demanding that pulses from the first 7.5 cm segment of a 42.5 cm depth glass Cerenkov detector exceed a 250 MeV threshold, a reduction of about a factor of four

was achieved in the background of pions under an electron peak at 5 GeV.⁴⁴

These authors also determined that use of this 250 MeV threshold resulted in acceptance of 98% of 4 GeV electrons and 90% of 2 GeV electrons, while rejecting about 87% of the 1-10 GeV pion spectrum they expected at large P_{\perp} from their ISR experiment. We conclude that a longitudinally segmented total absorption glass shower counter of this sort may be expected to discriminate pions from electrons in our expected 1-8 GeV/c spectrum of known-momentum pions and positrons (Fig. A.II.1) at the $2-3 \times 10^{-3}$ level provided the total counter thickness is adequate to capture essentially all of the shower produced by the e^{+} entering the front surface of the Pb-glass array. A CO_2 \checkmark Cerenkov counter (Appendix II) operates independently of the shower detector and is expected, a priori, to reduce the pion background another factor of 5 to permit us to attain an overall pion rejection at better than a 5×10^{-4} level. We note that the final electron detection configuration used by the authors of Ref.(44) also contained a gas \checkmark Cerenkov unit, replacing however, the initial glass counter segment with a thinner Fe-Absorber/Scintillator hodoscope layer.¹⁸

An additional consideration is the possibility that there can occur conspiratorial events in which, say, there may emerge both a fast pion which dumps an energy in the shower counter appropriate to its measured momentum and an accompanying π^0 which converts to trigger the gas counter and simulate a fast electron, also leaving enough energy in the front segment of the shower counter to exceed the electron threshold. It is desirable to segment as much as possible both the gas \checkmark Cerenkov and the glass \checkmark Cerenkov detectors to show up the transverse as well as the longitudinal structure of the overall event. This will, at a minimum, enable us to reject apparent electron signals which do not conform to the geometry expected from a simple extrapolation of tracks measured in the streamer chamber.

We propose to reconfigure the Pb-glass Cerenkov hodoscope system used by the Tufts-MIT-UMass-Cornell group to measure wide-angle Compton Scattering at 3-5 GeV. The basic detector will contain 60 glass blocks, arranged in 6 layers normal to the beam and oriented in alternating orthogonal directions as shown in Figure A.III.2. The effective area of acceptance is $(58.4 \times 58.4) \text{cm}^2$ or 0.341m^2 . (As we shall discuss later, it may be possible to double this acceptance with an 80 element configuration backed up by a Pb-scintillator system). The thickness of this counter will be 38.10 cm, or 13.4 rad. len. Above 5 GeV the contribution of leakage out the back to the energy resolution becomes comparable to the spread from intrinsic fluctuations.⁴⁵

An array of 1-1/2-inch wide scintillation counters is also available to cover the entire entrance aperture of the shower detector. It may prove necessary to place it in front of the shower array to veto interference from π^0 's produced at the target. Alternatively, it will permit the charged-pion rejection to be accomplished in the manner of Ref.(18), i.e. by causing entering particles to pass through a metal sheet radiator and the scintillator hodoscope, with pulse-height discrimination, before entering the glass counter.

To double the aperture of the shower detector, as suggested above, would require additional glass/PMT elements. Twenty elements identical to the 60 Tufts glass units are on loan to us from Professor J. B. Shafer of U Mass-Amherst, as do associated electronics. These would enable us to make two arrays of 40 counters in 4 layers, for a total area of $2 \times 58.4 \times 58.4 \text{cm}^2 = 0.68 \text{m}^2$. However, the depth of 8.9 rad. len. (or up to as much as 11 rad. len. if a pre-radiator is used), will not suffice to give adequate energy resolution for 4-5 GeV electrons. Since the capability to reject charge-exchanging π 's deteriorates with worsened

energy resolution, additional shower detectors behind the main array may be essential to make the improved acceptance worthwhile. We intend to use the shower detector available at Michigan State. The detector is composed of 20 modules of a lead scintillator sandwich system covering a total area of 60 cm wide by 1.25 m high. Each module consists of 16 alternating layers of lead and 1/8" thick scintillator sheets for a total of 7.6 radiation lengths. Since the lead scintillator sandwich system generally has worse energy resolution than a lead glass system, the trade-off for a larger solid angle coverage is possibly a reduction in capability to discriminate against π^+ . A detailed study will be undertaken, including if possible field tests, to establish the best configuration for optimum e^+/π^+ discrimination consistent with efficiency. The counter elements are all physically separate so that configurations may be readily altered.

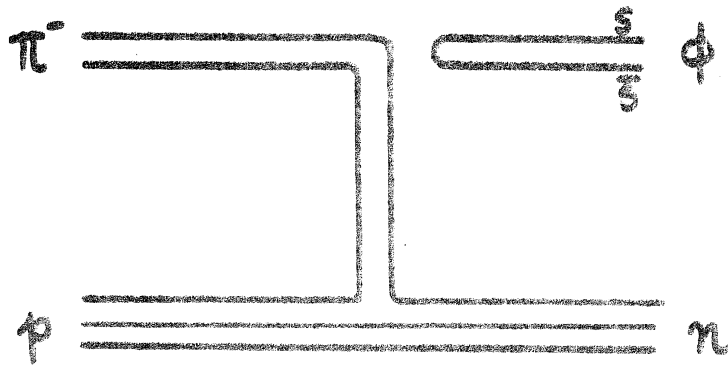
The Tufts Pb-glass Cerenkov counter system includes CAMAC-ADC readout, a controlling PDP-11/20 processor (with 24K of core, a disk pack, DECTape, printer, storage scope and a variety of interfacing circuitry, and LED-based calibration pulsing system under computer control, power supplies and monitors, and a variety of software for system calibration, monitoring and control. Except for mass data logging facilities-e.g. magnetic tapes-- the system can operate as a portable self-contained electron/photon spectrometer. A CAMAC-CAMAC interface facilitates communication with other computer systems having CAMAC Capability, and special interfaces can be built.

REFERENCES

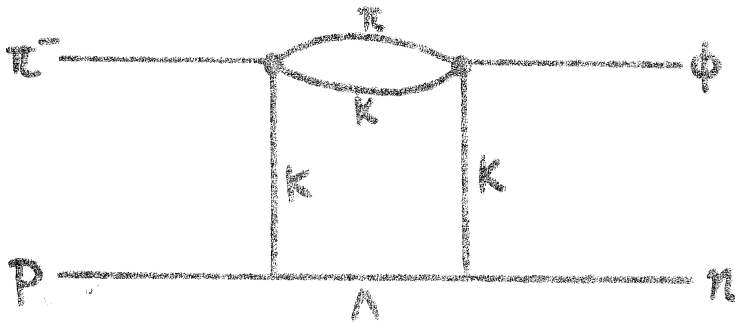
1. J. J. Aubert et al., Phys. Rev. Letters 33, 1404 (1974).
2. J. E. Augustin et al., Phys. Rev. Letters 33, 1406 (1974).
3. T. Appelquist, A. De Rujula, H. D. Politzer and S. L. Glashow, Phys. Rev. Letters 34, 365 (1975).
4. M. K. Gaillard, B. W. Lee, and J. L. Rosner, Rev. Mod. Phys. 47, 277 (1975).
5. J. J. Aubert et al., Phys. Rev. Letters 35, 416 (1975). S. C. C. Ting, Rapporteurs talk given at the EPS International Conference on High Energy Physics at Palermo, Sicily, Italy, June, 1975.
6. V. Hagopian et al., Phys. Rev. Letters 36, 296 (1976).
7. E. J. Bleser et al., Phys. Rev. Letters 35, 76 (1975).
8. C. Baltay et al., Phys. Rev. Letters 34, 1118 (1975).
9. D. S. Ayres, R. Diebold, A. F. Greene, S. L. Kramer, J. S. Levine, A. J. Pawlicki and A. B. Wicklund, Phys. Rev. Letters 32, 1463 (1974).
10. H. J. Lipkin, Phys. Letters 60B, 371 (1976).
11. R. A. Donald et al., Liverpool Preprint.
12. E. Berger and C. Sorensen, TH. 2149-CERN, 16 March, 1976.
13. D. Sivers, Phys. Rev. D11, 3253 (1975).
14. D. Sivers, RL-76-026-T.155, Rutherford Laboratory (1976).
15. For a comprehensive review on the current status of SU_3 , see Hadrons and SU_3 : A Critical Review, by N. P. Samios, M. Goldberg and B. T. Meadows. BNL 17851 (1973).
16. For an Excellent summary of the current status of prompt lepton production, see L. Lederman, 1975 International Symposium on Lepton and Electron Interactions, Stanford, p. 265.
17. L. Baum et al., Phys. Letters 60B, 485 (1976).
18. F. W. Busser et al., Phys. Letters 53B, 212 (1974).

19. L. B. Leipuner et al., Phys. Rev. Letters, 34, 103 (1975).
20. L. B. Leipuner et al., Phys. Rev. Letters 35, 1613 (1975).
21. D. Bintinger et al., Phys. Rev. Letters 35, 72 (1975).
22. J. P. Boymond et al., Phys. Rev. Letters 33, 112 (1974).
23. D. Buchholz et al., Phys. Rev. Letters 36, 932 (1976).
24. H. Kasha et al., Phys. Rev. Letters 36, 1007 (1976).
25. J. Ellis, M. K. Gaillard and D. V. Nanopoulos, Nucl. Phys. B100, 313 (1975).
26. J. Blietschau et al., Phys. Letters 60B, 207 (1976).
27. J. Canter et al., Search for Charmed Particles in 14.75 GeV/c $\bar{p}p$ Interactions, Tufts Preprint 76-1604 (1976).
28. G. Goldhaber et al., SLAC Preprint (1976).
29. G. Goldhaber, private communications.
30. Z. Ming Ma and B. Y. Oh, Comment on 'Search for More J Particles' MSU Preprint (1976).
31. G. J. Blamar et al., Phys. Rev. Letters 35, 346 (1975). See also K. T. McDonald, invited talk given at the APS Annual Meeting in New York, 1976.
32. R. D. Field and C. Quigg, FERMILAB-75/15-THY
33. V. Barger and R. J. N. Phillips, Phys. Rev. D12, 2623 (1975).
34. D. Pisello, Ph.D. Dissertation, Columbia University (1976), unpublished.
35. V. Blobel et al., Phys. Letters 59B, 88 (1975).
36. H. Hinterberger et al., Rev. of Sci. Inst. 41, 413 (1970).
37. M Benot, J. Litt and R. Meunier, Nucl. Inst. and Methods 105, 431 (1972).
38. E. L. Garwin and A. Roder, Nucl. Inst. and Methods 93, 593 (1971).
39. E. R. Hayes, R. A. Schluter and A. Tamo Saitis, ANL-6916 (1964).
40. Hugh H. Williams, Ph.D. Thesis SLA-142, Stanford University (1972).

- H. H. Williams, A. Kilert and D. W. G. S. Leith, Nucl Inst and Meth 105, 483 (1972).
41. G. B. Bowden et. al. " A Large Pressurized Cerenkov Counter", SLAC Preprint, unpublished.
 42. R. H. Siemann et al., Nucl. Inst. and Meth. 129, 427 (1975).
 43. B. J. Blumenfeld, L.M. Lederman, R. L. Cool and S. L. Segler, Nucl. Inst. and Meth. 97, 427 (1970).
 44. J. S. Beale et al., Nucl. Inst. and Meth. 117, 501 (1974).
 45. W. Atwood (SLAC) and F. Murphy (UCSB), Unpublished report.



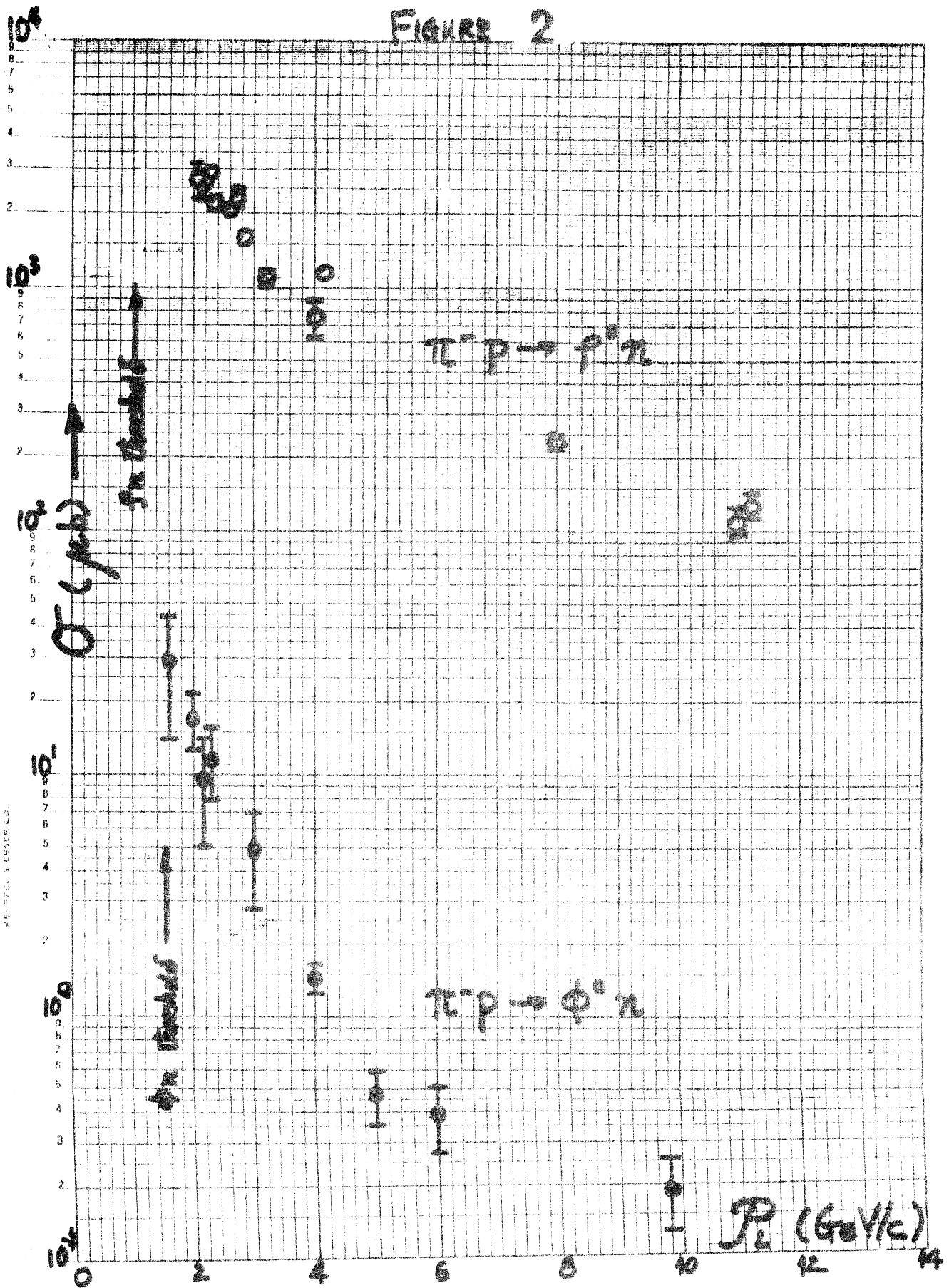
(a)



(b)

FIGURE 1

FIGURE 2



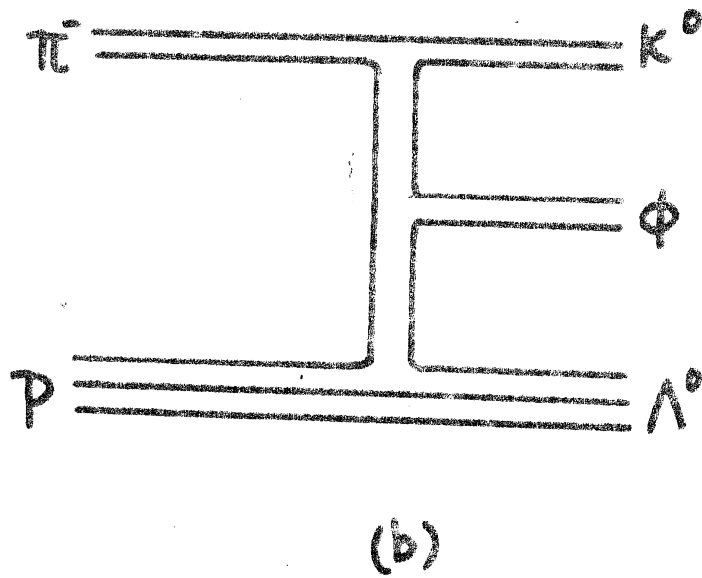
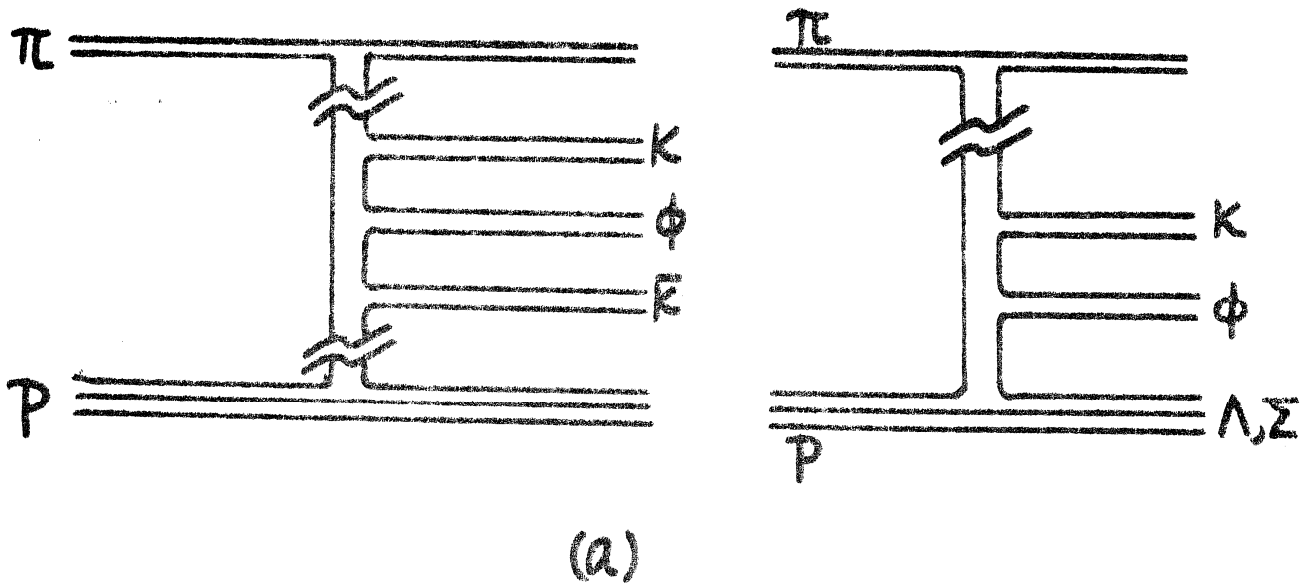


FIGURE 3

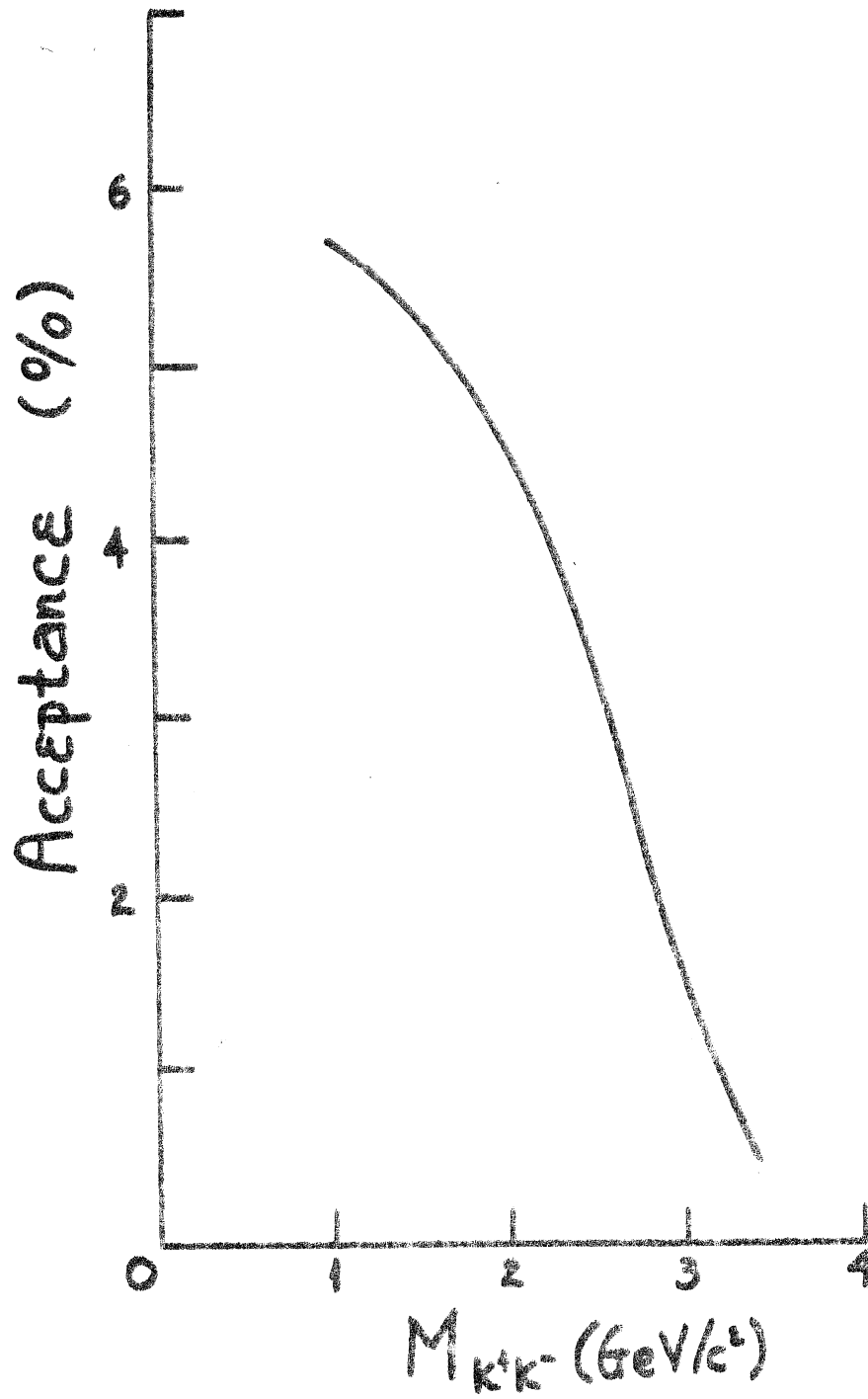


FIGURE 4

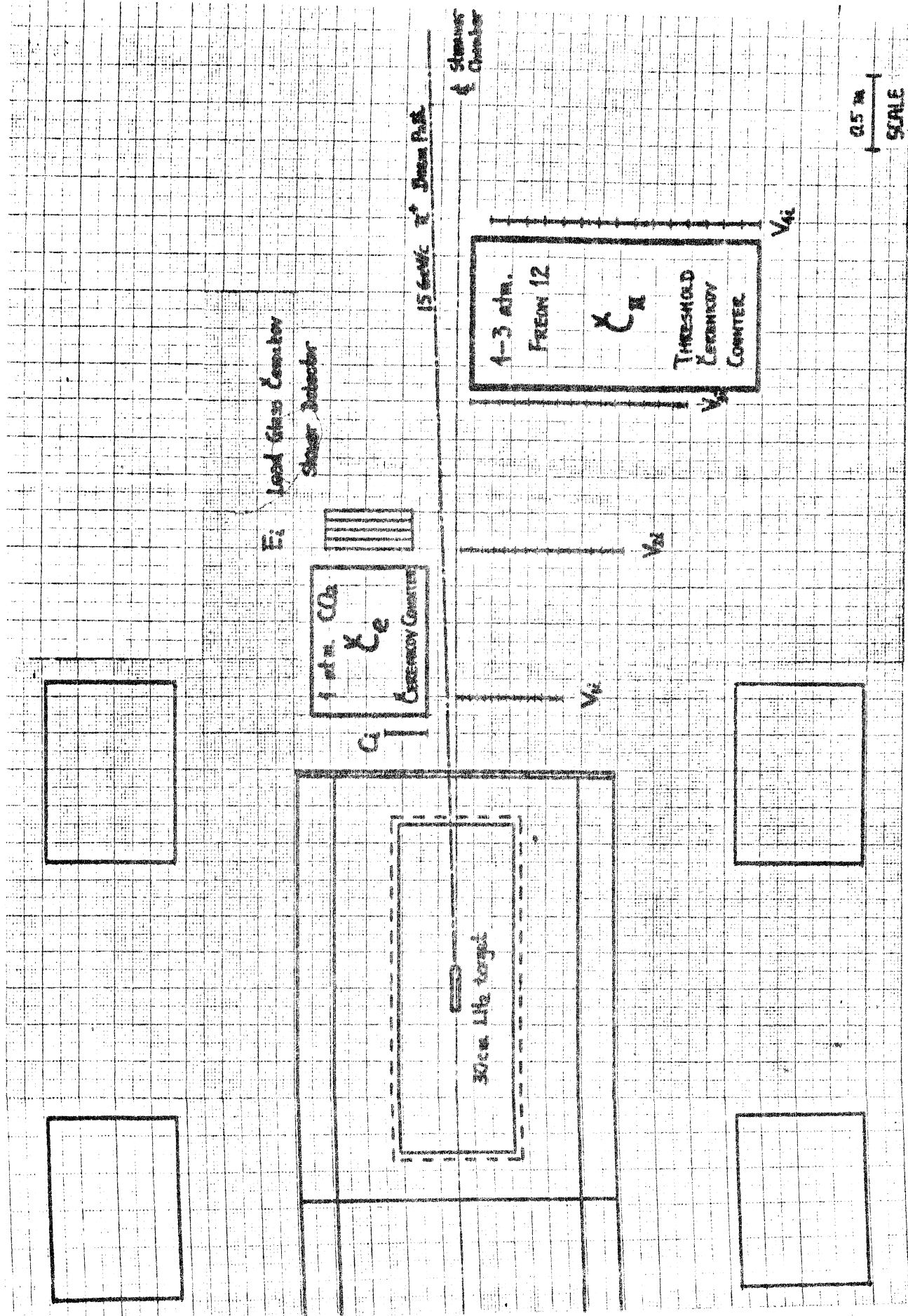
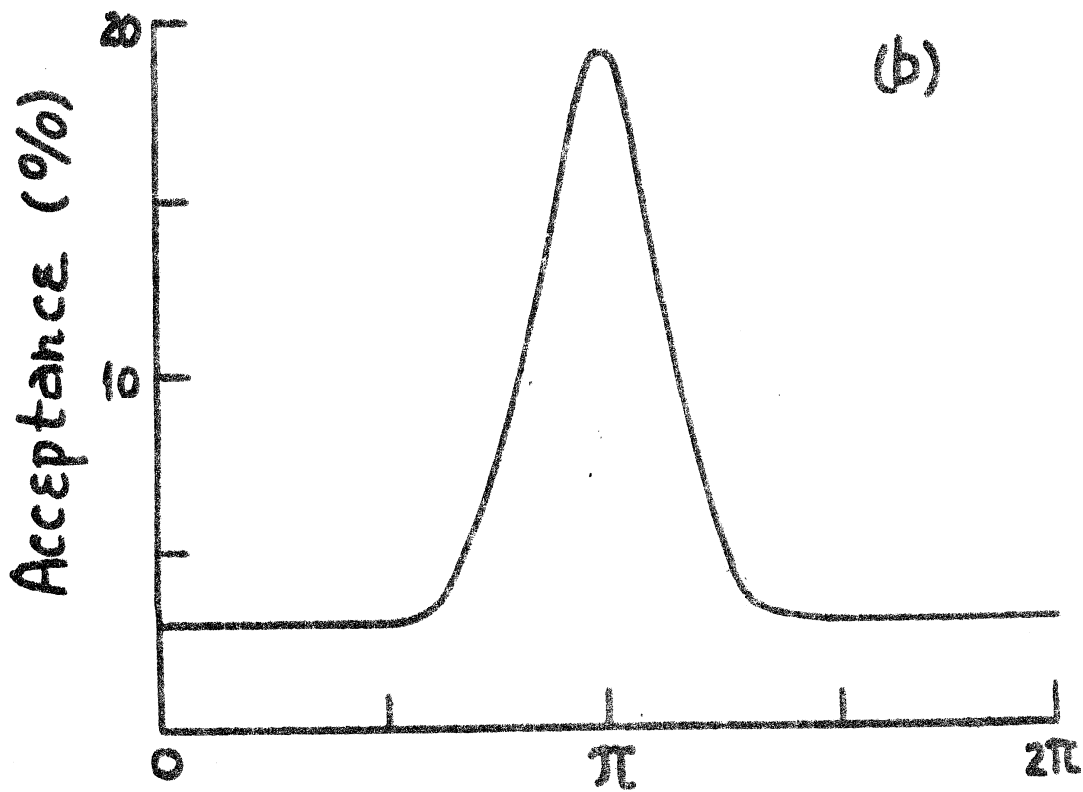
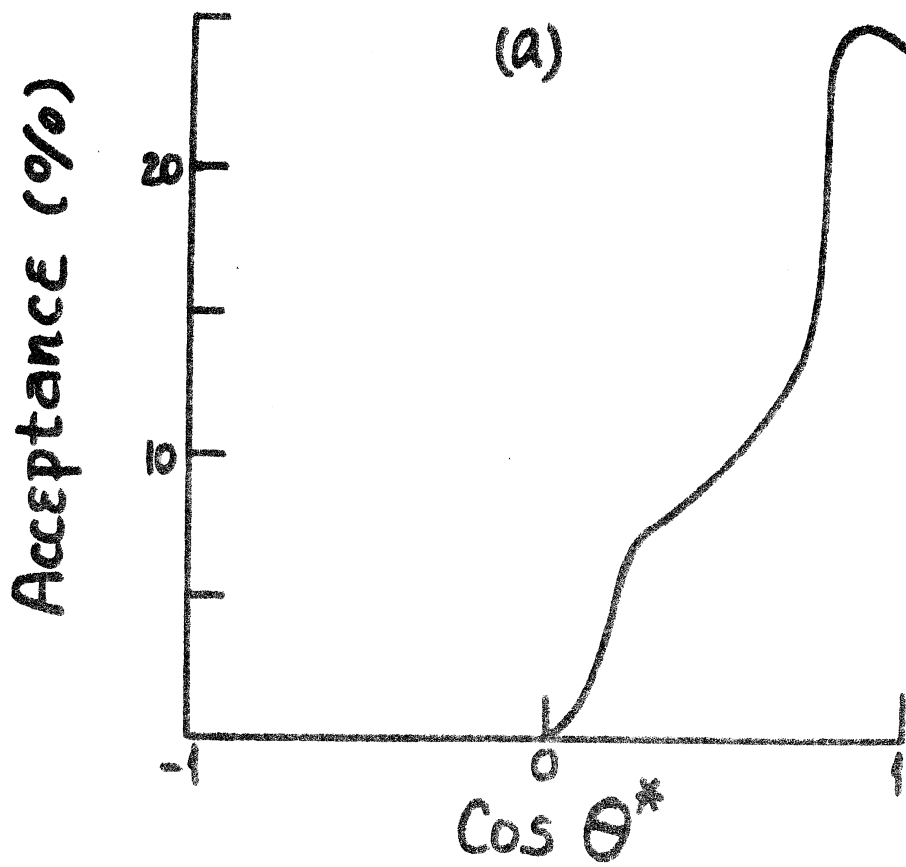
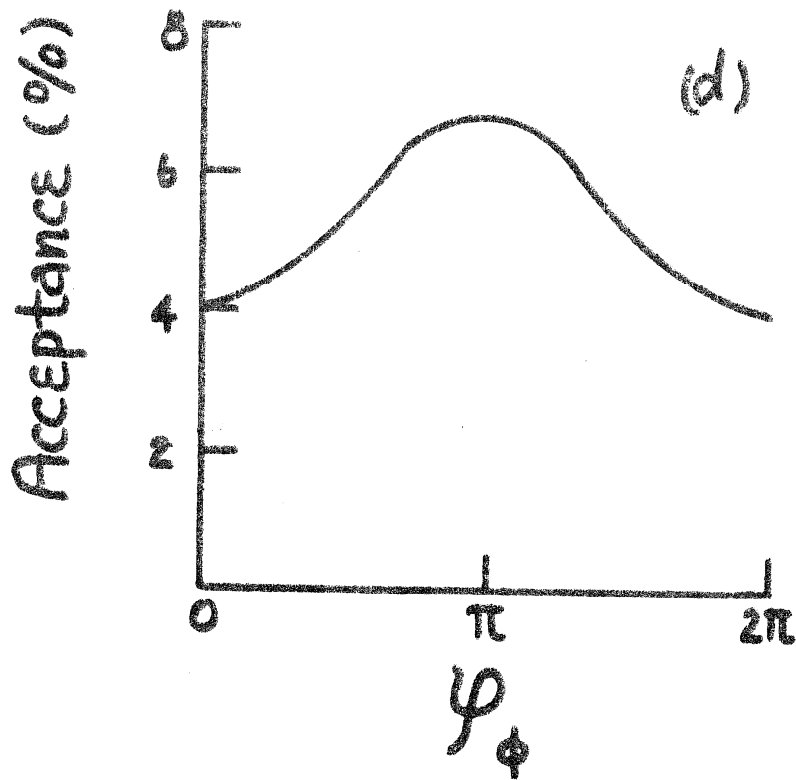
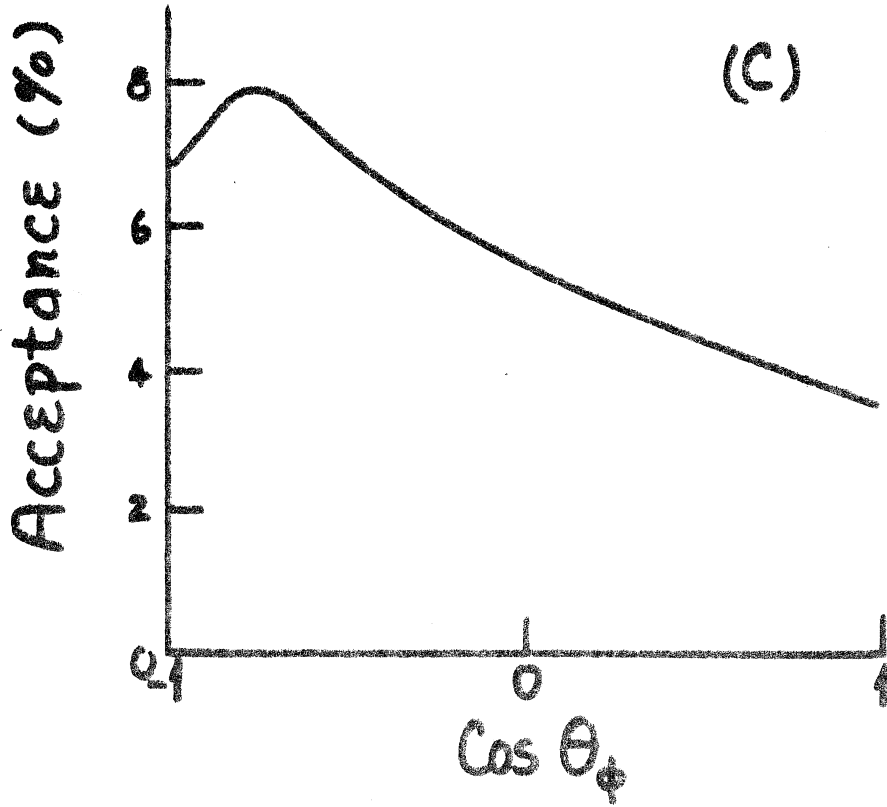


FIGURE 5



ϕ
FIGURE 6



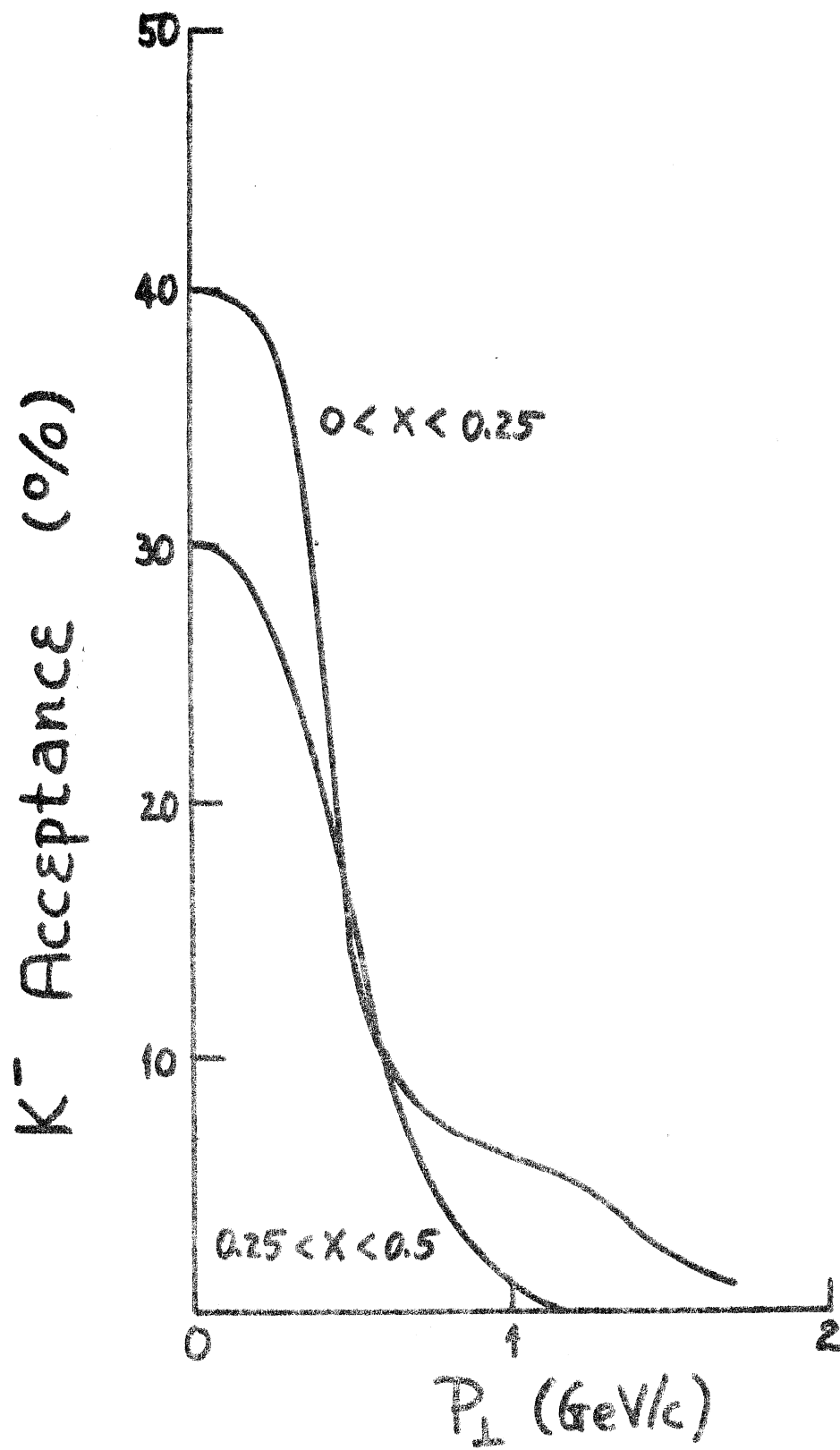


FIGURE 7

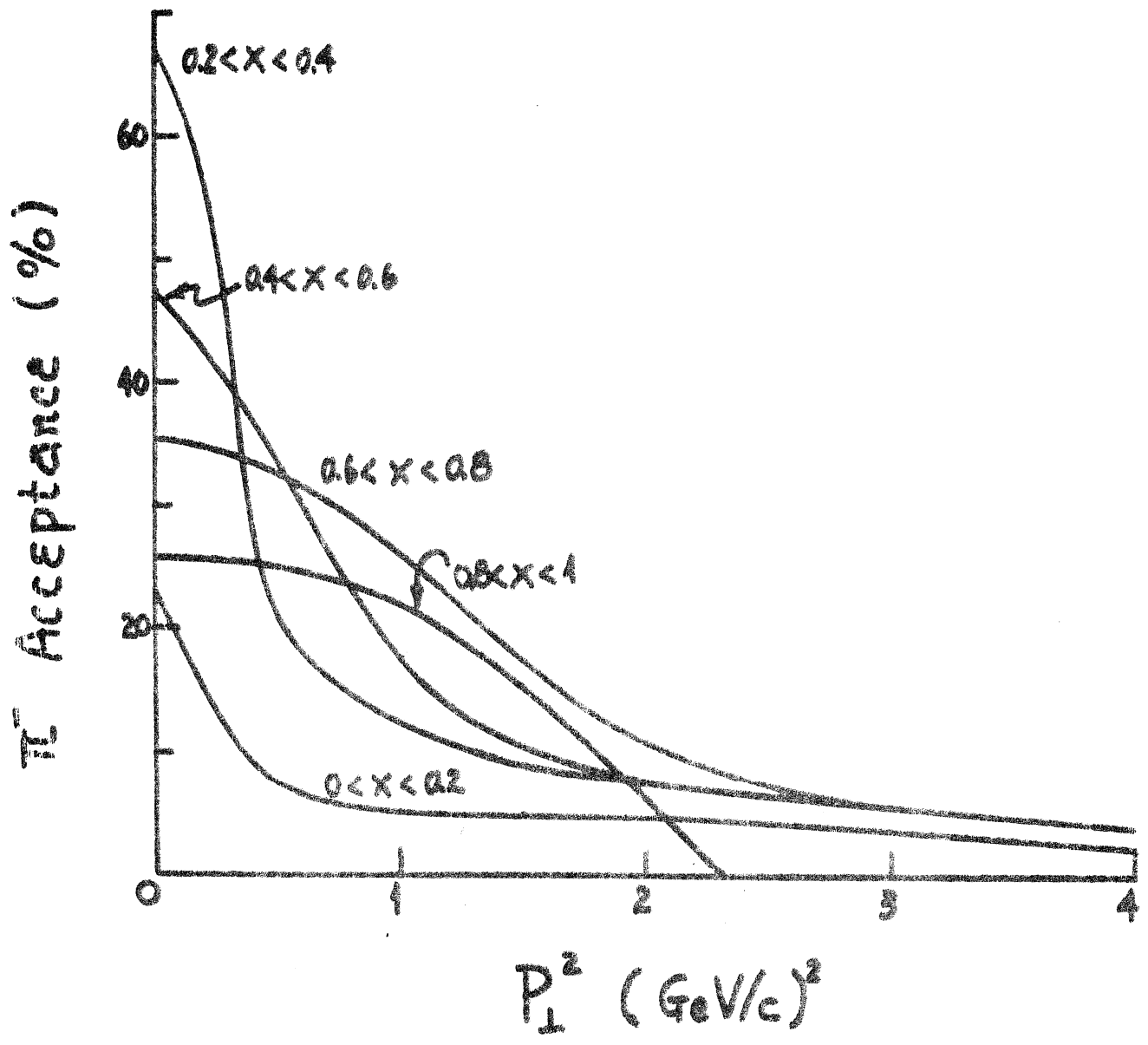


FIGURE 8

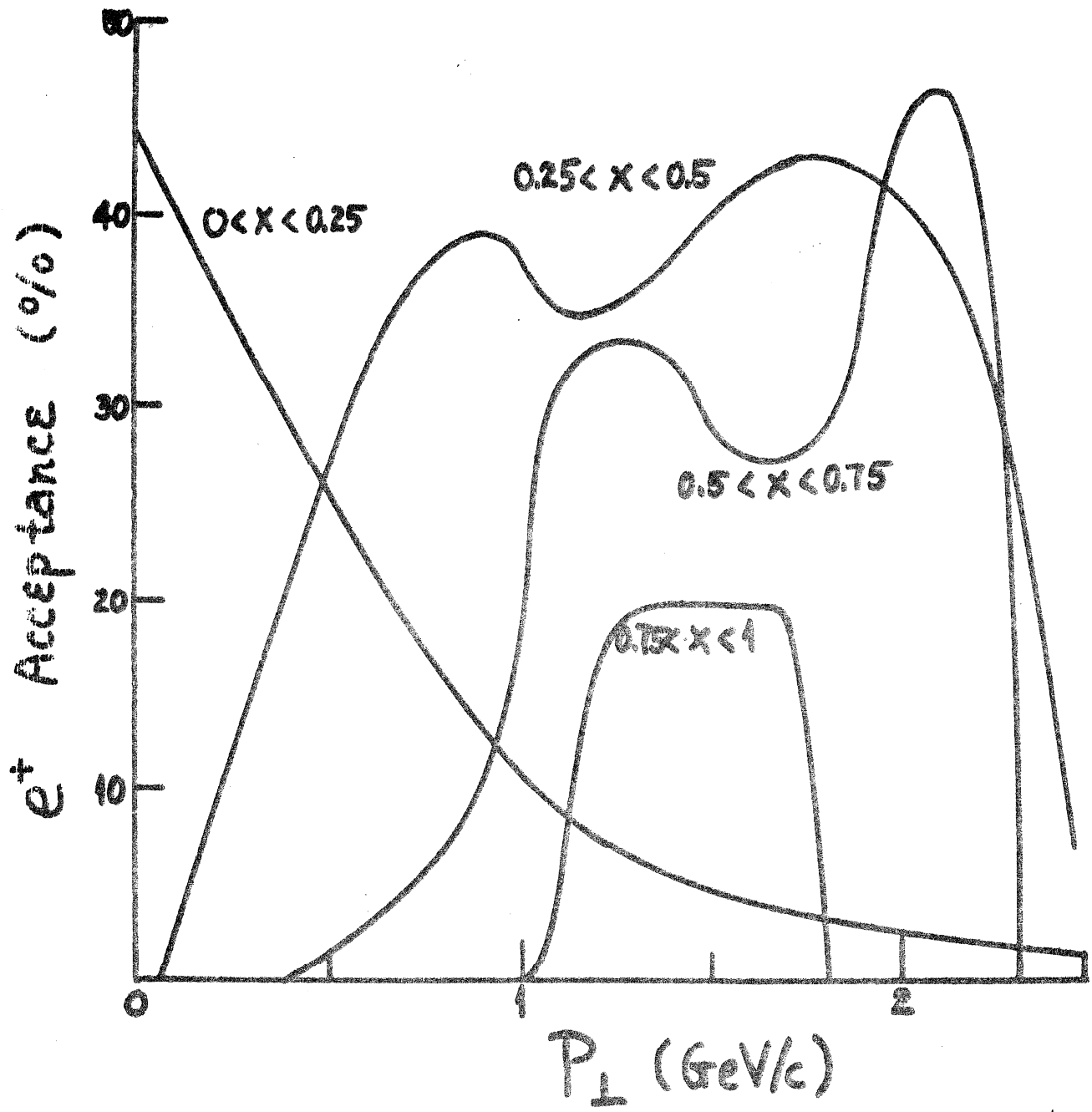


FIGURE 9

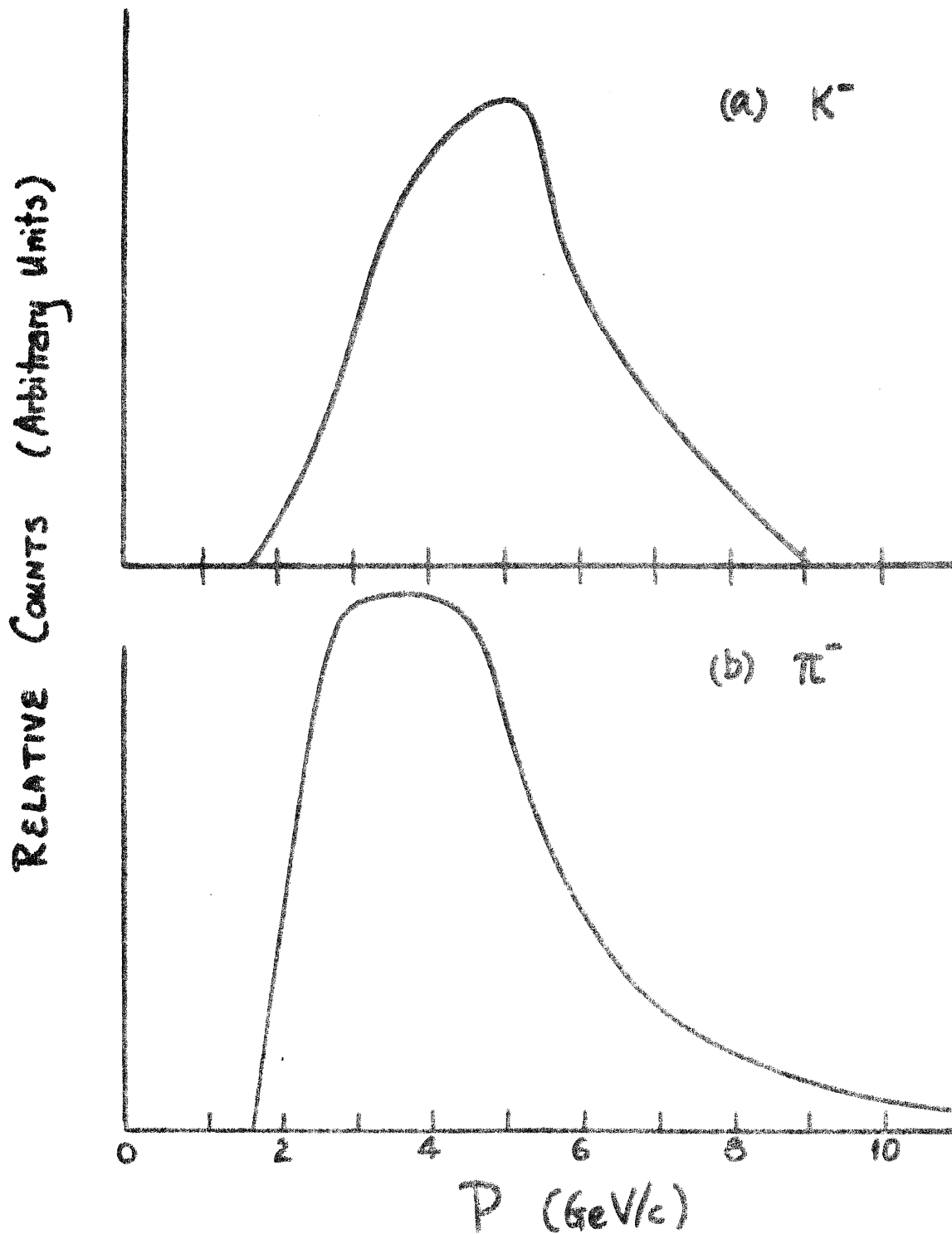
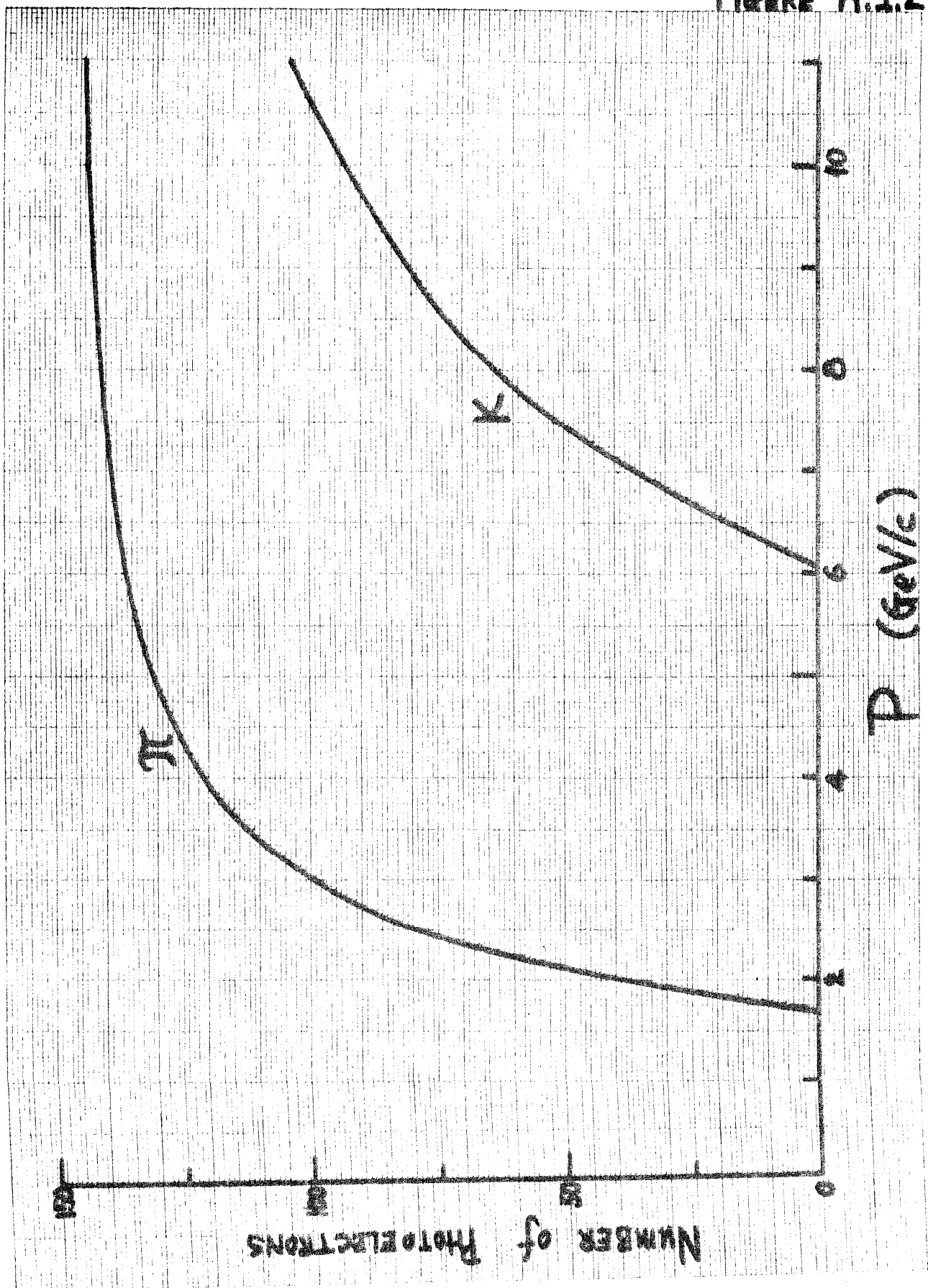


Figure A.I.1

FIGURE A.I.2



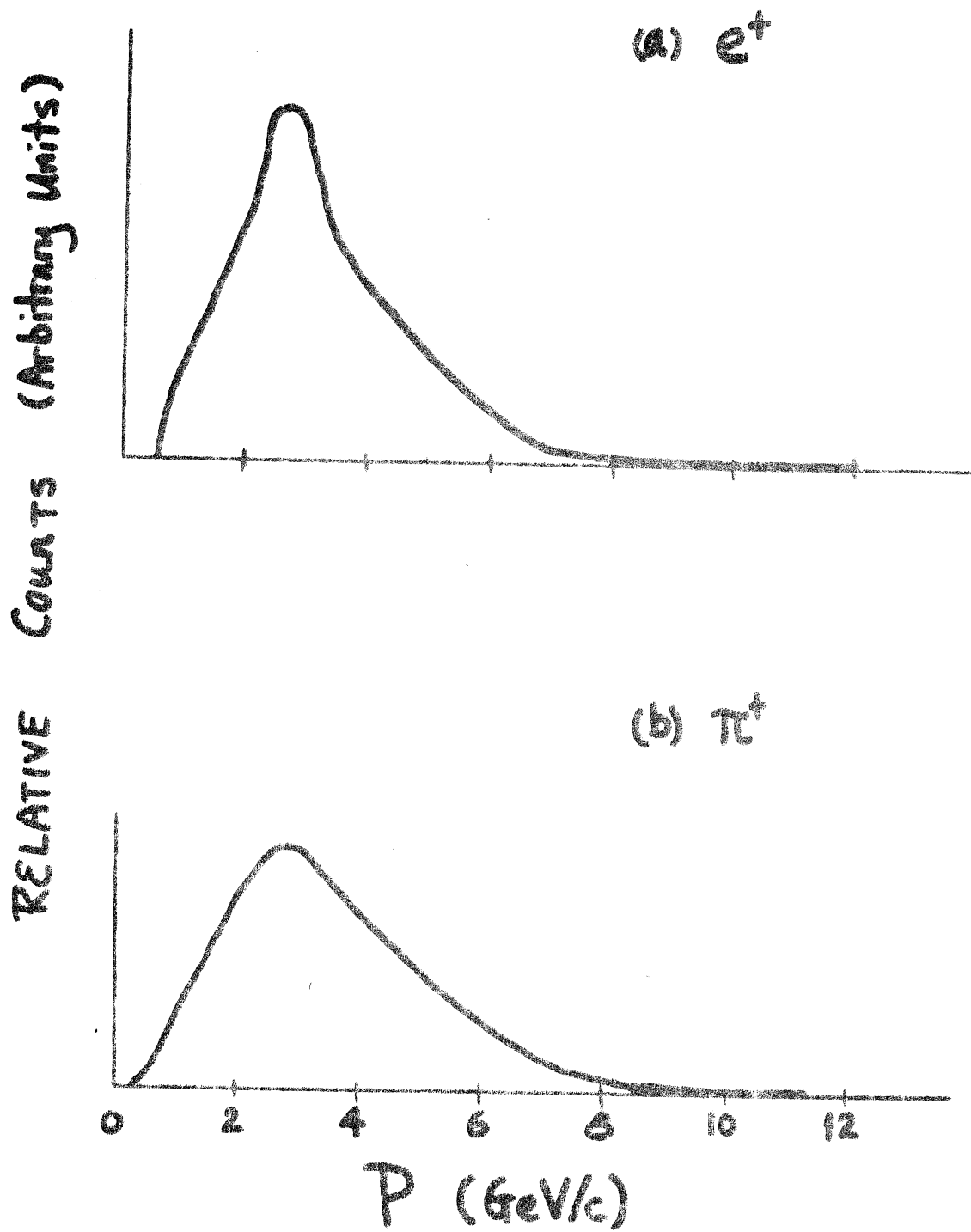


Figure A.II.1

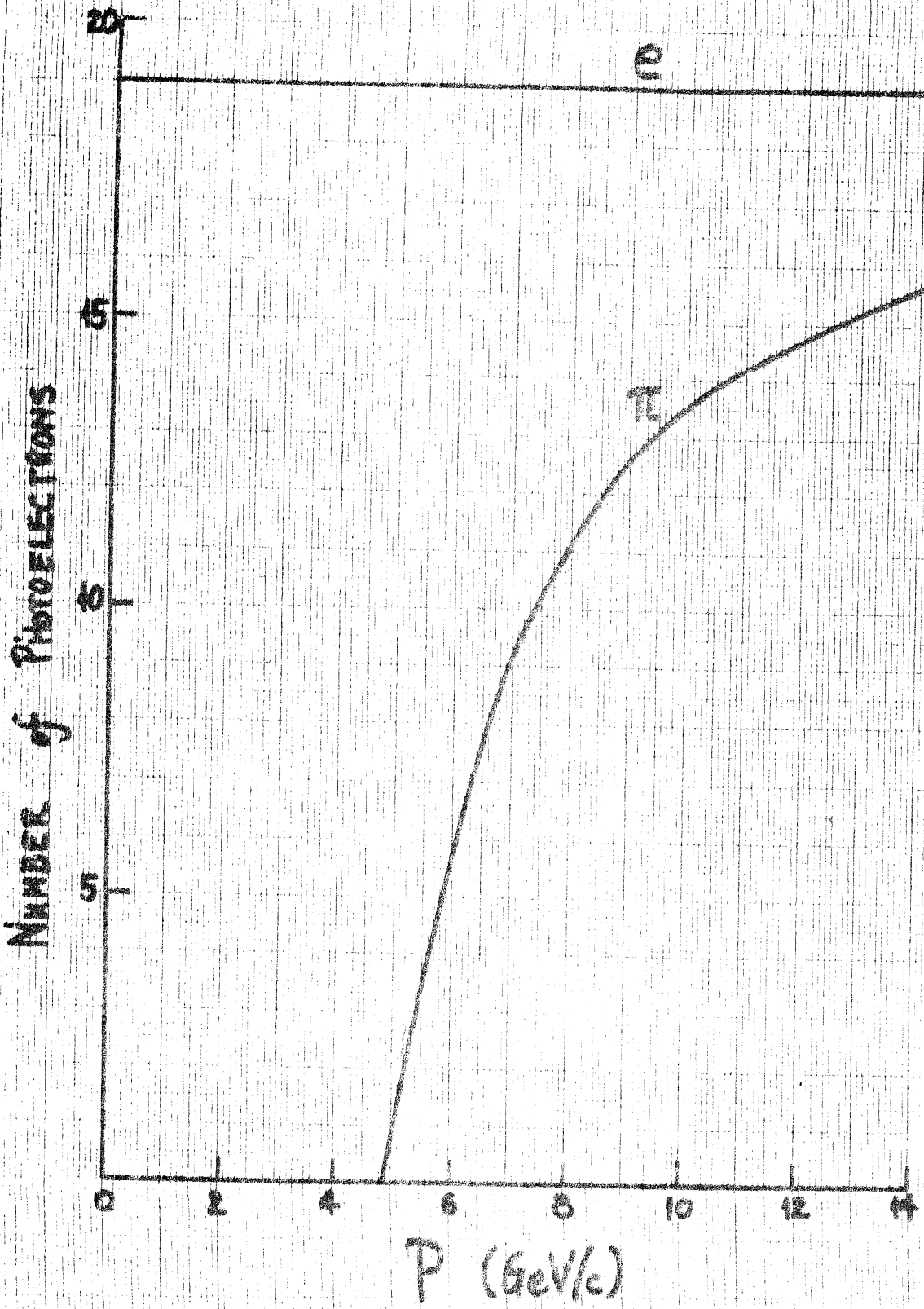


FIGURE A.II.2

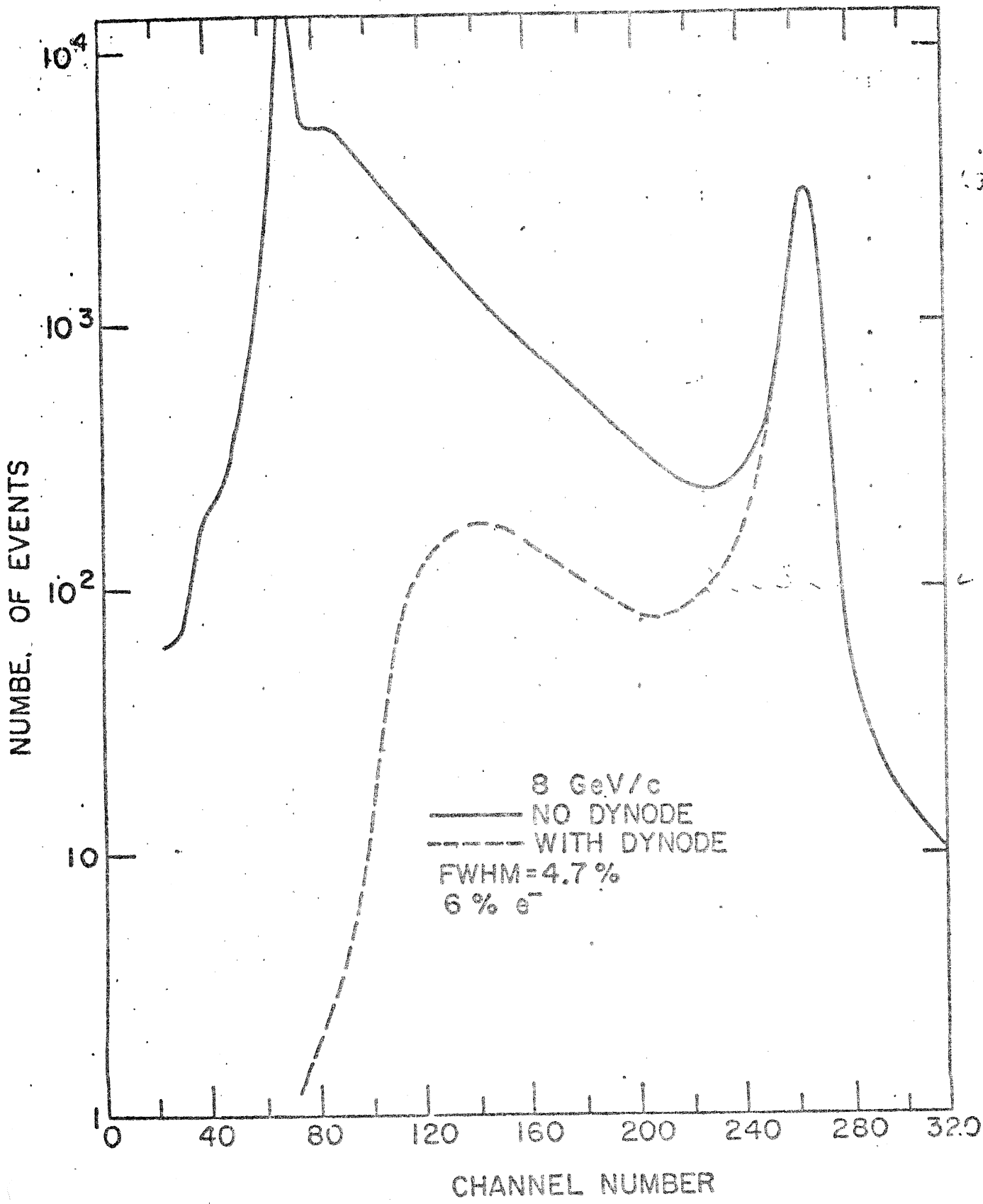
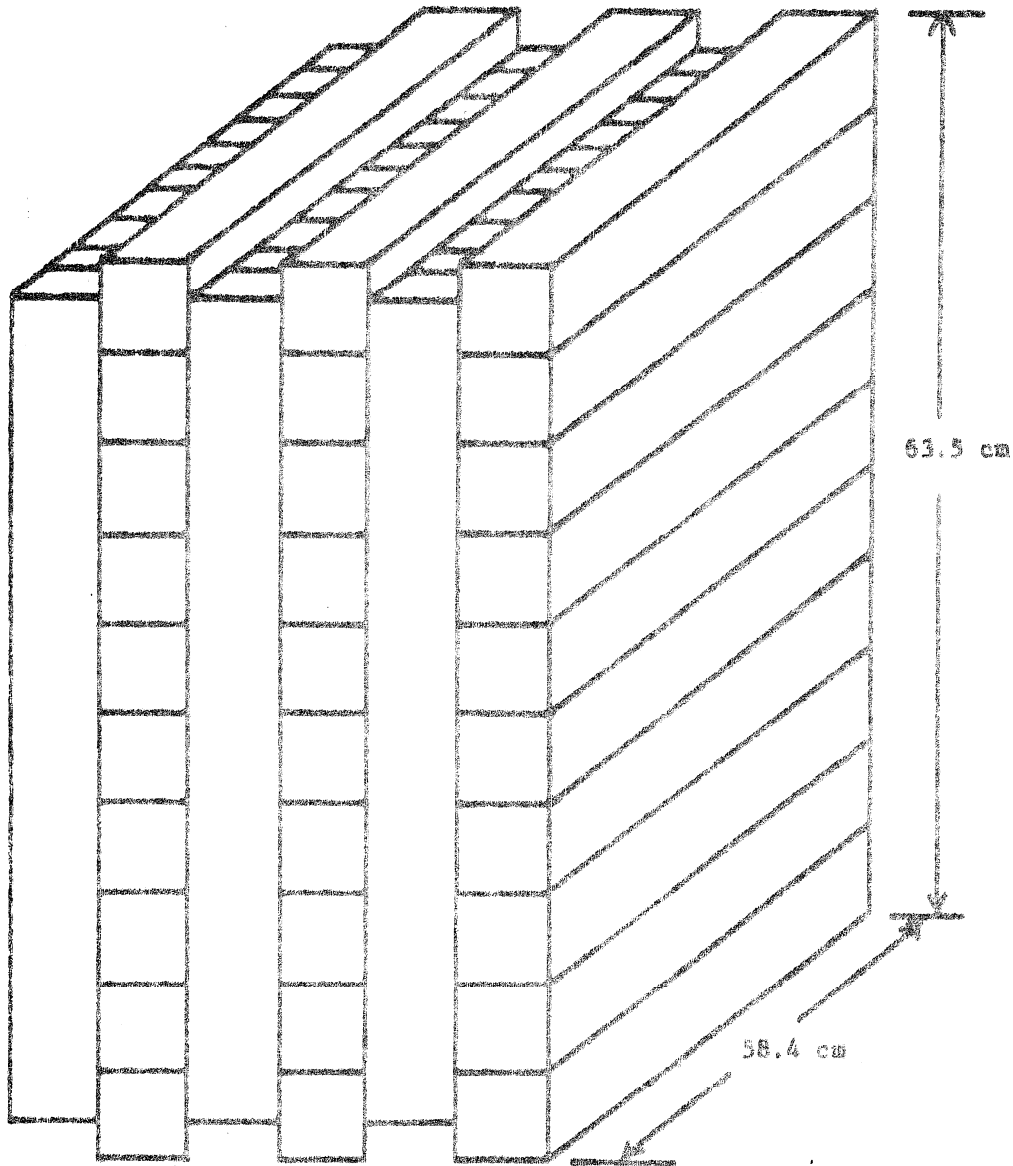


FIGURE A.II.1



LEAD GLASS SHOWER COUNTER (60 ELEMENT VERSION)

(PHOTOMULTIPLIERS, CALIBRATION LED'S, AND
LIGHT PIPES NOT SHOWN)

FIGURE A.II.2